Available online at www.sciencedirect.com
SCIENCE DIRECT®
Journal of Sound and Vibration 289 (2006) 745–778
JOURNAL OF SOUND AND VIBRATION
www.elsevier.com/locate/jsvi

Diffuse field transmission into infinite sandwich composite and laminate composite cylinders

Sebastian Ghinet[a,*], Noureddine Atalla[a], Haisam Osman[b]

[a]*Department of Mechanical Engineering, Université de Sherbrooke, 2500Boulevard Université, Sherbrooke, Que., Canada J1K 2R1*
[b]*The Boeing Company, 5301 Bolsa Avenue, Huntington Beach, CA 92647, USA*

Received 12 April 2004; received in revised form 7 February 2005; accepted 20 February 2005
Available online 5 May 2005

Abstract

This paper is concerned with the modelling of diffuse field transmission into composite laminate and sandwich composite infinite cylinders. Two models are presented and compared: Symmetrical Laminate composite and discrete thick laminate composite. The latter is shown to handle accurately, as a particular case, the first model, and the important case of sandwich composite shells. In both models, membrane, bending, transverse shearing as well as rotational inertia effects and orthotropic ply angle of the layers are considered. Starting from the dynamic equilibrium relations and stress–strain–displacement relations, a dispersion system is given in a wave approach context. Next, expressions for the matrix systems governing the structural impedance, critical frequencies and ring frequency are given. The developed equations are applied to the calculation of the diffuse field transmission of an infinite cylinder. Predictions with the presented models are compared to results presented in the literature for both laminate composite and sandwich composite configurations. They confirm the accuracy of both models and the general nature of the presented discrete thick laminate composite model.

*Corresponding author. Tel.: +1 819 821 8000x3773; fax: +1 819 821 7163.
E-mail address: sebastian.ghinet@usherbrooke.ca (S. Ghinet).

0022-460X/$ - see front matter © 2005 Elsevier Ltd. All rights reserved.
doi:10.1016/j.jsv.2005.02.028

1. Introduction

The laminate composite shells are a special class of modern structures, largely used in the aeronautics and aerospace industries. In addition to their inherent complexity related to the composite character of their nature, these structures are characterized by a significant total thickness and a large three-dimensional scale. In this study, we consider the case of acoustic transmission into a sandwich and/or composite laminated cylinders of infinite length, excited by a diffuse field. This class of problem has been presented, to a certain extent in several previous publications. In the context of the acoustic transmission through aeronautical structures, Koval [1] proposed an expression for the transmission coefficient of an orthotropic infinite shell using the displacement field of Nelson et al. [2]. The effects of membrane and bending were considered but transverse shearing and rotational inertia were neglected. The influence of orthotropic behaviour on the acoustic transmission was parametrically studied for the shell's elastic properties along circumferential and axial directions. The structure was excited by a plane wave in oblique incidence. The suggested solution was used for the study of the acoustic transmission in flight. The interior medium of the shell was considered non-resonant. Koval [3] later proposed an improved model for the acoustic transmission modelling of laminated composite infinite cylindrical shells excited by an oblique plane wave. Transverse shearing and rotational inertia were still neglected. The equilibrium dynamic relations of Bert et al. [4] employing a Kirchhoff-type displacement field were used. The orthotropic ply angle of the layers was considered. Blaise and Lesueur [5] investigated the same problems. They reported in particular some numerical errors in the work of Koval [1]. In their study, Blaise and Lesueur [5] used a Donnell–Mushtari's displacements field for orthotropic cylinders. Transverse shearing and rotational inertia were neglected. Moreover, they presented an extension of the excitation field to a diffuse field by associating two angles of incidence to the plane wave of excitation. However, the mathematical model validation and associated parameters study were entirely based on calculations of the oblique plane wave transmission loss. Only one result of the sound reduction index in diffuse field was presented; this result will be used in this paper for the validation of the presented models. Later, Blaise and Lesueur [6] proposed a model for the acoustic transmission of oblique incidence of multi-layered cylindrical shells. The orthotropic ply-angle was not considered. Finally, the same authors presented a more general model for the acoustic transmission through a 3-D orthotropic multi-layered infinite cylindrical shell [7]. Again, the layers were supposed to have orthotropic directions along the global coordinates of the shell. In a recent paper, Heron [8] proposed a wave approach for curved sandwich panels. His model uses a complete and mathematically coherent discrete layer theory for sandwich-type panels. The theory is developed for a singly curved sandwich made up of a bottom skin laminate, a shearing core, and a top skin laminate. This model is appropriate for the common case of thin skin-laminated composite sandwich shells. For sandwich shells having thick or limp (compared to the core) skins the model is approximate. Moreover, the model of Heron [8] does not accommodate the laminated thick composite shells (i.e., non-sandwich) where the layers' physical properties (Young's modulus, Transverse shear modulus, and mass density) are of similar or relatively close values.

This paper describes an alternative, simple but accurate, modelling of the transmission loss through infinite composite cylinders. Both laminate composite and sandwich composite will be modelled. The transverse shear and orthotropic angle of such a laminate are considered. In the

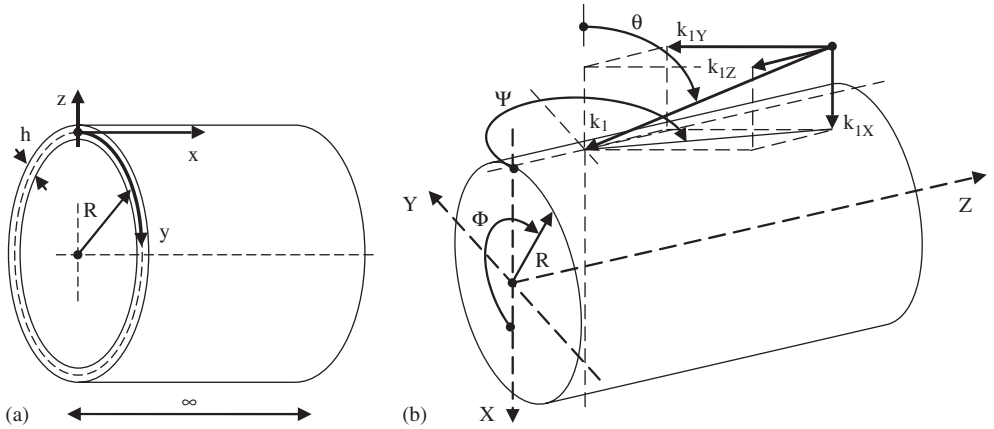

Fig. 1. (a) The laminated composite shell coordinates and (b) The excitation field notations and cylindrical coordinates system.

first part, the fundamental relations of force equilibrium are expressed in the curvilinear coordinates system represented in Fig. 1a. Two mathematical approaches to model composite structures are presented. The first structural class is limited to symmetrical laminated composite shells. The physical properties of the laminas' composing the panel are smeared out through the thickness and the panel is assumed to have a unique global displacement field for any lamina. The second structural class is applicable to general thick laminate composite shells. For any layer an own displacement field and dynamic equilibrium system is defined. This approach is valid for both general laminate (symmetrical and unsymmetrical) and sandwich composite shells. In particular, expressions are given to compute the ring frequency, the critical frequencies and mechanical impedance of the studied structures. Using numerical examples, the two models are validated and compared in the case of the diffuse field transmission of an infinite composite cylinder (non-resonant interior). Moreover, the discrete laminate model and the Heron's model [8] are also compared in the case of a sandwich shell. The proposed laminate composite discrete layer theory is validated experimentally for the case of a finite sandwich curved panel.

2. Mathematical models

2.1. Geometry and coordinates system

The presented models are based on the Flüge description of the strain–displacements field in a curved layer, as given by Leissa [9]. Fig. 1a represents the laminated composite shell geometrical configuration, where R is the curvature radius and h is the total thickness. The equations of motion are expressed in the curvilinear coordinate system shown in Fig. 1a. The excitation and radiated fields are expressed in the cylindrical coordinate system represented in Fig. 1b. The transmission loss is expressed in these two reference coordinates systems using the associated transformation relations (see Eqs. (38), Section 6). This approach of using two different reference coordinates is of interest since it allows taking advantage of the simplicity of mathematical

development in curvilinear coordinates as well as to correctly model the influence of the acoustic fields by a formulation in cylindrical coordinates. Mathematically, the curvature radius is defined as the coordinate of the neutral surface of the cylinder.

2.2. Symmetric laminate composite curved shells

For a point M belonging to the symmetrically laminated composite shell, the displacement field is defined by the Mindlin model where both bending and transverse shear effects are considered:

$$\begin{aligned} u(x,y,z) &= u_0(x,y) + z\varphi_x(x,y), \\ v(x,y,z) &= v_0(x,y) + z\varphi_y(x,y), \\ w(x,y,z) &= w_0(x,y). \end{aligned} \tag{1}$$

The displacement field variables in relations (1) are shown in Fig. 2. Geometrically, the shell is considered to be of infinite extent in the axial (x) direction and thus the origin for both x and y is arbitrary. Nevertheless, the origin for the z-axis is defined on a reference surface passing through the middle thickness of the shell.

For any lamina of the shell, Flüge's theory [9] is used to describe the strain–displacement relations

$$\begin{aligned} \varepsilon_x &= u_{,x} + z\varphi_{x,x}, \\ \varepsilon_y &= \left(v_{,y} + \frac{w}{R} + z\varphi_{y,y}\right)\frac{1}{1+z/R}, \\ \gamma_{xy} &= (v_{,x} + z\varphi_{y,x}) + (u_{,y} + z\varphi_{x,y})\frac{1}{1+z/R}, \end{aligned}$$

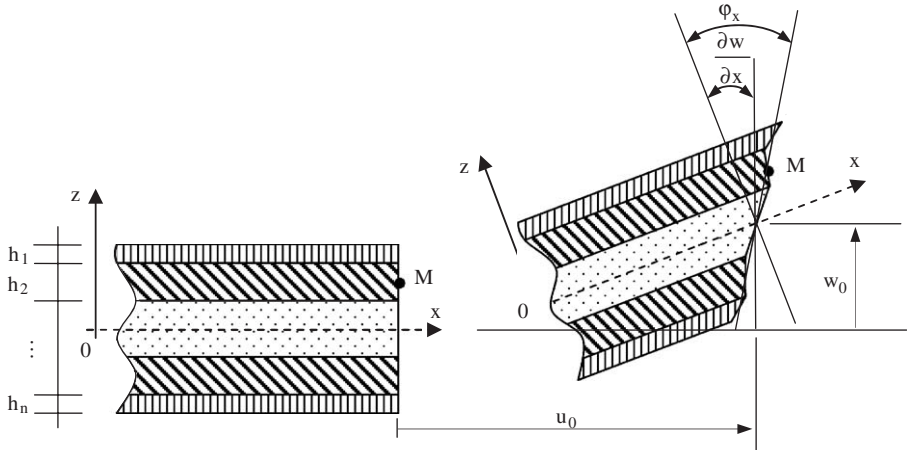

Fig. 2. The laminated composite shell displacements field.

$$\gamma_{xz} = w_{,x} + \varphi_x,$$
$$\gamma_{yz} = w_{,y} + \varphi_y - (v + z\varphi_y)\frac{1}{R+z}. \tag{2}$$

The resultant stress forces and moments of the laminate are defined in Appendix A (A.1 and A.2).

The differential equations of dynamic equilibrium are derived from stress forces and moments equilibrium relations in the x, y and z directions [9,10]. The layers are not considered as discrete elements, but their effects are smeared-out through the thickness. This results in five equilibrium equations for the shell. In the following equations, all inertial terms, membrane, bending as well as transverse shear effects are considered:

$$N_{x,x} + N_{yx,y} = \left(m_s + \frac{I_{z2}}{R}\right)u_{,tt} + \left(\frac{I_z}{R} + I_{z2}\right)\varphi_{x,tt},$$
$$N_{y,y} + N_{xy,x} + \frac{Q_y}{R} = \left(m_s + \frac{I_{z2}}{R}\right)v_{,tt} + \left(\frac{I_z}{R} + I_{z2}\right)\varphi_{y,tt},$$
$$Q_{x,x} + Q_{y,y} - \frac{N_y}{R} = \left(m_s + \frac{I_{z2}}{R}\right)w_{,tt},$$
$$M_{x,x} + M_{yx,y} - Q_x = I_z\left(\varphi_{x,tt} + \frac{u_{,tt}}{R}\right) + I_{z2}u_{,tt},$$
$$M_{xy,x} + M_{y,y} - Q_y = I_z\left(\varphi_{y,tt} + \frac{v_{,tt}}{R}\right) + I_{z2}v_{,tt}. \tag{3}$$

The transverse shear-stress forces Q_x and Q_y, the in-plane stress forces N_x, N_y, N_{xy}, N_{yx} and the stress moments M_x, M_y, M_{xy}, M_{yx} are defined in Appendix A (A.4–A.6). The inertial terms derived in the equilibrium equations (3) are expressed in Appendix A (A.7). Note that the rotational inertia I_{z2} is zero for symmetrically laminated composite panels.

The dynamic equilibrium equations of the shell can be rewritten, using Eqs. (3) and (A.4)–(A.6) with appropriate algebraic manipulations, as presented in Appendix A (A.12). Relations (A.12) are then expressed in terms of an in-plane and bending displacement–rotation vector $\langle e\rangle$ defined as

$$\langle e\rangle = \langle u\ v\ w\ \varphi_x\ \varphi_y\rangle^{\mathrm{T}}, \tag{4}$$

where the superscript "T" denotes the transpose of a vector.

The differential system of equations (A.12) is then allowed to have harmonic solutions of the form

$$\langle e\rangle = \{e\}\exp(\mathrm{j}k_x x + \mathrm{j}k_y y - \mathrm{j}\omega t), \tag{5}$$

where k_x and k_y are the structural wave number components in the x and y directions defined as

$$k_x = k_c\cos\varphi,$$
$$k_y = k_c\sin\varphi \tag{6}$$

with φ the heading direction of the structural wave number k_c.

Using the solution form (5), the system equations of motion (A.12) is expressed in the form of a generalized polynomial complex eigenvalue problem

$$k_c^2[A_2]\{e\} - \mathrm{i}k_c[A_1]\{e\} - [A_0]\{e\} = 0, \tag{7}$$

where $\mathrm{i} = \sqrt{-1}$ and $[A_0], [A_1], [A_2]$ are real matrices of dimension 5×5 defined in Appendix A (A.13). Assuming $\lambda = \mathrm{i}k$, problem (7) can be expressed in the form

$$\lambda^2[A_2]\{e\} + \lambda[A_1]\{e\} + [A_0]\{e\} = 0. \tag{8}$$

Eq. (8) is a second-order complex polynomial eigenvalue problem. It is preferable to transform it into a first-order system

$$\lambda \begin{bmatrix} A_1 & A_2 \\ A_2 & 0 \end{bmatrix} \begin{Bmatrix} e \\ \lambda e \end{Bmatrix} - \begin{bmatrix} -A_0 & 0 \\ 0 & A_2 \end{bmatrix} \begin{Bmatrix} e \\ \lambda e \end{Bmatrix} = \begin{Bmatrix} 0 \\ 0 \end{Bmatrix}, \tag{9}$$

so as to obtain a generalized eigenvalue problem. Relation (9) has 10 complex conjugate eigenvalues (five conjugate pairs) and represents the dispersion relations of the laminated composite shell. The problem is expressed in terms of λ and its solutions represent the structural wave numbers: propagating or evanescent, in two opposite directions. The propagating wave solution must satisfy $\lambda = \pm \mathrm{i}k$ (purely imaginary) while the evanescent wave solution corresponds to the mathematically real eigenvalue of the problem (with an infinitely small imaginary component).

2.3. Discrete thick laminate composite curved shells

The second model is more general. It is based on a discrete theory and allows for both thick laminate composites and sandwich shells. The displacement field of any discrete layer "i" of the panel is still of Mindlin's type

$$\begin{aligned} u^i(x, y, z) &= u_0^i(x, y) + z\varphi_x^i(x, y), \\ v^i(x, y, z) &= v_0^i(x, y) + z\varphi_y^i(x, y), \\ w^i(x, y, z) &= w_0^i(x, y). \end{aligned} \tag{10}$$

The layered constitution is considered asymmetrical as represented in Fig. 3a. The origin for the z-axis is defined on a reference surface passing through the middle thickness of the shell. Rotational inertia, in-plane, bending as well as transverse shearing effects are accounted for in each layer. Also, orthotropic ply angle is used for any layer.

For any layer of the shell, Flüge's theory [9] is used to describe the strain–displacement relations (2). The resultant stress forces and moments of any layer are defined in Appendix A (A.1 and A.2). Considering that any layer "i" is made up from "N^i" laminas, the theory developed in Section 2.1 applies here for any layer.

There are three interlayer forces between any two layers, as represented in Fig. 3b. The total number of interlayer forces is $3(N-1)$, where N is the number of layers. For any layer "i" there

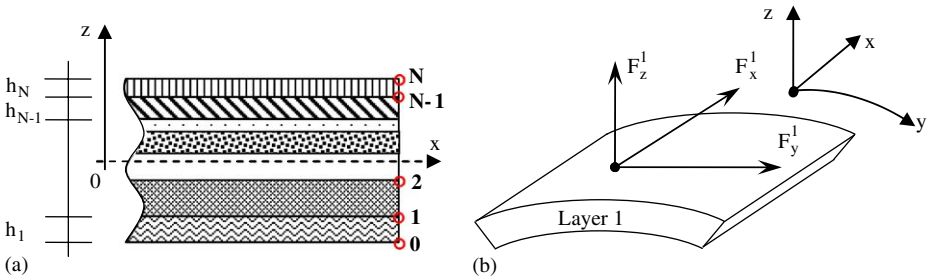

Fig. 3. The discrete laminated composite shell thickness constitution (a) and interlayer forces (b).

are five equilibrium equations:

$$
\begin{aligned}
&N^i_{x,x} + N^i_{yx,y} + F^i_x - F^{i-1}_x = \left[\left(m_s + \frac{I_{z2}}{R}\right)u_{,tt} + \left(\frac{I_z}{R} + I_{z2}\right)\varphi_{x,tt}\right]^i,\\
&N^i_{y,y} + N^i_{xy,x} + \frac{Q^i_y}{R} + F^i_y - F^{i-1}_y = \left[\left(m_s + \frac{I_{z2}}{R}\right)v_{,tt} + \left(\frac{I_z}{R} + I_{z2}\right)\varphi_{y,tt}\right]^i,\\
&Q^i_{x,x} + Q^i_{y,y} - \frac{N^i_y}{R} + F^i_z - F^{i-1}_z = \left[\left(m_s + \frac{I_{z2}}{R}\right)w_{,tt}\right]^i,\\
&M^i_{x,x} + M^i_{yx,y} - Q^i_x + z^i F^i_x - z^{i-1}F^{i-1}_x = \left[I_z\left(\varphi_{x,tt} + \frac{u_{,tt}}{R}\right) + I_{z2}u_{,tt}\right]^i,\\
&M^i_{xy,x} + M^i_{y,y} - Q^i_y + z^i F^i_y - z^{i-1}F^{i-1}_y = \left[I_z\left(\varphi_{y,tt} + \frac{v_{,tt}}{R}\right) + I_{z2}v_{,tt}\right]^i.
\end{aligned}
\tag{11}
$$

The external and internal surfaces of the shell are considered stress-free so that $F^0_x = F^0_y = F^0_z = 0$ and $F^N_x = F^N_y = F^N_z = 0$. The expressions of the transverse shear-stress forces, the in-plane stress forces, the inertial terms and the stress moments are presented in Appendix A (A.4–A.7). For any layer, the dynamic equilibrium equations can be rewritten, using Eqs. (11) and (A.4)–(A.6) with appropriate algebraic manipulations, as presented in Appendix B (B.2).

There are three relations of interlayer continuity of displacements for each of the $N-1$ interlayer surfaces as follows:

$$
\begin{aligned}
&u^i(x,y,z_i) = u^i_0(x,y) + z_i\varphi^i_x(x,y) = u^{i+1}_0(x,y) + z_i\varphi^{i+1}_x(x,y) = u^{i+1}(x,y,z_i),\\
&v^i(x,y,z_i) = v^i_0(x,y) + z_i\varphi^i_y(x,y) = v^{i+1}_0(x,y) + z_i\varphi^{i+1}_y(x,y) = v^{i+1}(x,y,z_i),\\
&w^i(x,y,z_i) = w^i_0(x,y) = w^{i+1}_0(x,y) = w^{i+1}(x,y,z_i).
\end{aligned}
\tag{12}
$$

The problem has $5N + 3(N-1)$ variables regrouped in two vectors; an in-plane and bending displacement–rotation vector $\{U\}$ and an interlayer forces vector $\{F\}$:

$$
\begin{aligned}
\{U\} &= \{u^1; v^1; w^1; \varphi^1_x; \varphi^1_y; u^2; v^2; w^2; \varphi^2_x; \varphi^2_y; \cdots u^N; v^N; w^N; \varphi^N_x; \varphi^N_y\}^{\mathrm{T}},\\
\{F\} &= \{F^1_x; F^1_y; F^1_z; F^2_x; F^2_y; F^2_z; \cdots F^{N-1}_x; F^{N-1}_y; F^{N-1}_z\}^{\mathrm{T}}.
\end{aligned}
\tag{13}
$$

The associated $5N + 3(N-1)$ equations are composed of five equations of dynamic equilibrium for each of the N layers plus three equations of interlayer continuity of displacements for each of

the $N-1$ interlayer surfaces. As an example, the problem of a three layers (laminate composite or sandwich composite) panel has 21 variables and 21 equations.

To solve for the dispersion relations, the system of equations (B.2) is expressed in terms of a hybrid vector $\{e\}$ defined as

$$\{e\} = \left\{ \begin{array}{c} U \\ F \end{array} \right\}. \tag{14}$$

Assuming a harmonic solution (5), the system is expressed in the form of a generalized polynomial complex eigenvalue problem:

$$k_c^2[A_2]\{e\} - \mathrm{i}k_c[A_1]\{e\} - [A_0]\{e\} = 0, \tag{15}$$

where $\mathrm{i} = \sqrt{-1}$ and $[A_0]$, $[A_1]$, $[A_2]$ are real square matrices (in the absence of damping) of dimension $5N + 3(N-1)$ defined in Appendix B (B.3). Relation (15) has $2(5N + 3(N-1))$ complex conjugate eigenvalues and represents the dispersion relations of the laminated composite shells. As an example, a sandwich composite shell has a dispersion relation of 42nd order.

The transverse shearing is known to become influent in middle frequencies when the panel is thick. Its influence is not negligible as could be the rotational inertia's in some cases. The rotational inertia becomes influent for thick panels and must be considered especially when high frequency accuracy is an aim. And yet, the rotational inertia is physically and numerically important here in assuming the equilibrium in the discrete layered relations of motion. Ignoring rotational inertia could result, in most sandwich structures cases, in large numerical errors due to mathematical singularities.

3. Ring frequency

The following applies to both models. However, the presentation will be limited to the symmetrical laminate for its simplicity. At the ring frequency, the shell displacement is characterized by a breathing mode shape. It follows that, the derivatives of the in-plane and bending displacement–rotation vector $\{e\}$ along x and y directions are equal to zero. Eq. (7) simplifies to

$$[A_{01}]\{e\} = \omega_r^2[A_{02}]\{e\}, \tag{16}$$

which represents a generalized eigenvalues problem with $[A_{01}]$ and $[A_{02}]$, real matrices of dimension 5×5 defined as follows:

$$[A_{01}] = \begin{bmatrix} 0 & 0 & 0 & 0 & 0 \\ 0 & -\dfrac{F_{44}}{R^2} + \dfrac{H_{44}}{R^3} & 0 & \dfrac{F_{45}}{R} & \dfrac{F_{44}}{R} - \dfrac{H_{44}}{R^2} \\ 0 & 0 & -\dfrac{A_{22}}{R^2} + \dfrac{B_{22}}{R^3} & 0 & 0 \\ 0 & \dfrac{F_{45}}{R} & 0 & -F_{55} - \dfrac{H_{55}}{R} & -F_{45} \\ 0 & \dfrac{F_{44}}{R} - \dfrac{H_{44}}{R^2} & 0 & -F_{45} & -F_{44} - \dfrac{H_{44}}{R} \end{bmatrix}, \tag{17}$$

$$[A_{02}] = \begin{bmatrix} -m_s & 0 & 0 & -\frac{I_z}{R} & 0 \\ 0 & -m_s & 0 & 0 & -\frac{I_z}{R} \\ 0 & 0 & -m_s & 0 & 0 \\ -\frac{I_z}{R} & 0 & 0 & -I_z & 0 \\ 0 & -\frac{I_z}{R} & 0 & 0 & -I_z \end{bmatrix}. \tag{18}$$

The numerical solution of Eq. (16) leads to the ring frequency $\omega_r = 2\pi f_r$ of the shell. Symbolically, the solution of the generalized eigenvalues problem (16) leads to

$$\omega_r = \sqrt{\left(A_{22} - \frac{B_{22}}{R}\right)\frac{1}{R^2 m_s}}. \tag{19}$$

We observe that the ring frequency is independent of the rotational inertia and the bending stiffness. It is also independent of the membrane effects in the axial direction of the shell. As in the case of isotropic shells, the ring frequency of the laminate composite cylindrical shells depends just on the curvature radius, the mass per unit area and the membrane stiffness in the circumferential direction. A similar procedure to Eq. (16) is used for the discrete thick laminate theory.

4. Critical frequencies

By analogy with plates, the critical frequencies of the curved shell are given by the particular solution of the dispersion (7) at coincidence; that is when the structural wavenumber matches the acoustic wavenumber:

$$\begin{aligned} &k_c^2[A_2]\{e\} - \mathrm{i}k_c[A_1]\{e\} - [A_0]\{e\} = 0, \\ &k_0 = k_c = \omega/c_0. \end{aligned} \tag{20}$$

In the classical case of thin isotropic panel, the critical frequency is given by

$$f_c = \frac{c_0^2}{2\pi}\sqrt{\frac{m_s}{D}}, \tag{21}$$

where D is the bending stiffness, m_s is the mass per unit area and c_0 is the speed of sound in air.

In the case of a laminated composite panel ($R \to \infty$), the critical frequency is computed numerically from Eq. (20) using $[A_0] = [A_{01}] - \omega^2[A_{02}]$:

$$\omega_c^2\left[\frac{[A_2]}{c_0^2} + [A_{02}]\right]\{e\} - \mathrm{i}\omega_c\frac{[A_1]}{c_0}\{e\} - [A_{01}]\{e\} = 0, \tag{22}$$

which is a second-order polynomial eigenvalues problem with $[A_{01}]$, $[A_{02}]$, $[A_1]$ and $[A_2]$ defined by the relations (17), (18) and (A.13). Assuming $\lambda_c = \mathrm{i}\omega_c$, Eq. (22) can be expressed

in the form

$$\lambda_c^2\left[\frac{[A_2]}{c_0^2}+[A_{02}]\right]\{e\}+\lambda_c\frac{[A_1]}{c_0}\{e\}+[A_{01}]\{e\}=0. \tag{23}$$

Or equivalently

$$\lambda_c\begin{bmatrix}\dfrac{[A_1]}{c_0} & \dfrac{[A_2]}{c_0^2}+[A_{02}]\\ [I] & [0]\end{bmatrix}\begin{Bmatrix} e\\ \lambda_c e\end{Bmatrix}=\begin{bmatrix}-[A_{01}] & [0]\\ [0] & [I]\end{bmatrix}\begin{Bmatrix} e\\ \lambda_c e\end{Bmatrix}, \tag{24}$$

to obtain a generalized eigenvalue problem, where $[I]$ is the identity matrix and [0] a null matrix of dimension 5×5. This problem has 10 complex conjugate eigenvalues. The critical frequency corresponds to a solution which satisfies the condition $\lambda_c(\varphi)=\pm i\omega_c$, purely imaginary. The critical frequency of the laminated composite panel can be written as

$$f_c(\varphi)=\mp\frac{i\lambda_c(\varphi)}{2\pi}. \tag{25}$$

It is known [11] that an isotropic panel has a critical frequency while for an orthotropic panel; a critical frequency region is defined. In the same manner, the limits of the critical frequency region for the laminated composite panels are defined by $f_{c1}=f_c(\varphi=0)$ and $f_{c2}=f_c(\varphi=\pi/2)$. A similar procedure is used for the discrete thick laminate theory.

5. Structural impedance

The acoustic structural impedance of the laminate composite shell is computed numerically when the structure vibration is forced by a plane wave at oblique incidence. The acoustic wave number trace is imposed to propagate in the structure and the relation (9) is rewritten in the form of a linear equations system as follows:

$$(k_c^2[A_2]-ik_c[A_1]-[A_0])\cdot\{e\}=\{b\}, \tag{26}$$

where $\{b\}=\langle 0,0,p,0,0\rangle^t$, p is the amplitude of the acoustical pressure of excitation and k_c is the trace of the acoustic wave number. The associated displacement vector $\{e\}$ is the numerical solution of the linear system (26). The acoustic structural impedance of the shell is then expressed as the ratio of the acoustic wave pressure $p=b(3)$ and the normal velocity $\dot{w}$ of the shell as

$$Z_s(k_c,\varphi)=\frac{b(3)}{i\omega e(3)}. \tag{27}$$

The matrices $[A_0]$, $[A_1]$ and $[A_2]$, in Eq. (26), are complex. The stiffness coefficients (A.8b) considered in these matrices has an imaginary part governed by the structural damping coefficients of the constituent layers. Once again, a similar approach is used for the discrete thick laminate theory.

6. Diffuse field transmission loss

As an application of the above formulations, this section considers the acoustic transmission in a diffuse field through laminate composite and sandwich composite infinite cylinders. The interior acoustic medium of the shell is considered non-resonant, therefore only one transmitted wave is accounted for in the development of the expression of the transmission coefficient [6,11]. The incident plane wave on the structure is defined by two angles, as represented in Fig. 1b.

The external and internal acoustic mediums of the shell are considered identical and are defined by the density of the fluid $\rho_{01} = \rho_{02}$ and the speed of sound $c_{01} = c_{02}$. The development of the acoustic transmission coefficient expression is carried in the cylindrical coordinates system suggested in Fig. 1b. All waves are assumed to have the same dependence in the axial direction of the shell. The cylinder is considered to be of infinite length.

The incident plane wave is represented by

$$\begin{aligned} p_i &= P_i \exp(\mathrm{i}(\omega t - k_{1Z}Z - k_{1X}X - k_{1Y}Y)) \\ &= P_i \exp(\mathrm{i}(\omega t - k_{1Z}Z - k_{1X}R\cos\Phi - k_{1Y}R\sin\Phi)), \end{aligned} \tag{28}$$

where k_X, k_Y and k_Z are the acoustic wave number components defined as

$$\begin{aligned} k_{1X} &= k_1 \cos\theta, \\ k_{1Y} &= k_1 \sin\theta \sin\Psi, \\ k_{1Z} &= k_1 \sin\theta \cos\Psi \end{aligned} \tag{29}$$

and $k_1 = k_2 = \omega/c_0$ are the acoustic wave numbers of the excitation and reception media.

Using Eq. (29), it is seen that

$$\begin{aligned} k_{1X}R\cos\Phi + k_{1Y}R\sin\Phi &= k_1 R\cos\theta\cos\Phi + k_1 R\sin\theta\sin\Psi\sin\Phi \\ &= \frac{k_1\cos\theta}{\cos\beta} R\left[\cos\beta\cos\Phi + \cos\beta\frac{\sin\theta}{\cos\theta}\sin\Psi\sin\Phi\right] \\ &= k_W R[\cos\beta\cos\Phi + \sin\beta\sin\Phi] \\ &= k_W R\cos(\beta + \Phi) \end{aligned} \tag{30}$$

where the notations

$$k_W = \frac{k_1\cos\theta}{\cos\beta} \quad \text{and} \quad \mathrm{tg}\,\beta = \mathrm{tg}\,\theta\sin\Psi$$

are used.

It results in the incident pressure expression:

$$p_i = P_i \exp(\mathrm{i}(\omega t - k_{1Z}Z - k_W R\cos(\beta + \Phi))). \tag{31}$$

Expanding the relation (31) in cylindrical harmonics [12] gives

$$\begin{aligned} p_i &= P_i \exp(\mathrm{i}(\omega t - k_{1Z}Z))\exp(-\mathrm{i}k_W R\cos(\beta + \Phi)) \\ &= P_i \exp(\mathrm{i}(\omega t - k_{1Z}Z))\sum_{n=0}^{\infty} \varepsilon_n(-\mathrm{i})^n J_n(k_W R)\cos(n(\beta + \Phi)), \end{aligned} \tag{32}$$

where ε_n is the Neumann factor given by

$$\varepsilon_n = \begin{cases} 1 & \text{for } n = 0, \\ 2 & \text{for } n = 1 \end{cases} \tag{33}$$

and J_n is the Bessel function of the first kind and nth order.

The incident wave on the structure p_i gives a reflected wave p_{ref} in the excitation medium and a transmitted wave p_t in the interior medium of the shell. These two waves are written in the form [6]

$$p_{\text{ref}} = \exp(\mathrm{i}(\omega t - k_{1Z}Z)) \sum_{n=0}^{\infty} A_n \varepsilon_n (-\mathrm{i})^n H_n^1(k_W R) \cos(n(\beta + \Phi)), \tag{34}$$

$$p_t = \exp(\mathrm{i}(\omega t - k_{2Z}Z)) \sum_{n=0}^{\infty} B_n \varepsilon_n (-\mathrm{i})^n H_n^2(k_W R) \cos(n(\beta + \Phi)), \tag{35}$$

where $k_{1Z} = k_{2Z}$, A_n is the reflected wave amplitude, B_n is the transmitted wave amplitude, H_n^1 and H_n^2 are the Hankel functions of the first and second kind and nth order.

The modal transmission coefficient of the shell is proven to be given by Blaise and Lesueur [6]

$$\tau(\omega, \theta, \Psi) = \sum_{n=0}^{\infty} \frac{2\varepsilon_n}{R \cdot k_1 \cos\theta} \frac{\mathrm{Re}\{Z_n^R\}\mathrm{Re}\{Z_n^t\}}{|Z_n^R + Z_n^t + Z_n^S|^2}, \tag{36}$$

$$Z_n^R = -\mathrm{i}\omega \frac{\rho_0}{k_1 \cos\theta} \frac{H_n^2(k_W R)}{H_n'^2(k_W R)}, \quad Z_n^t = \mathrm{i}\omega \frac{\rho_0}{k_2 \cos\theta} \frac{H_n^1(k_W R)}{H_n'^1(k_W R)}, \tag{37}$$

where Z_n^R is the modal impedance of the reflected wave, Z_n^t is the modal impedance of the transmitted wave and $Z_n^S = Z_s(k_c, \varphi)$ is the structural modal impedance of the shell given by Eq. (27) for the laminate composite shell or the equivalent relation for the discrete thick laminate theory.

Next, the forced wave number is expressed in the cylindrical coordinate system of the acoustic field. Two expressions which connect the curvilinear and the cylindrical coordinates systems are obtained

$$\varphi = \arcsin\left(\frac{n}{k_c R}\right) \quad \text{and} \quad k_c = \sqrt{\left(\frac{n}{R}\right)^2 + k_{1Z}^2}. \tag{38}$$

The diffuse field sound reduction index of the shell is thus expressed as

$$\begin{aligned} \mathrm{TL}(\omega) &= -10\log_{10}(\tau_d(\omega)) + 10\log_{10}(\pi), \quad \text{with} \\ \tau_d(\omega) &= \frac{\int_0^{2\pi}\int_{\theta_{\min}}^{\theta_{\max}} \tau(\omega, \theta, \Psi)\,\mathrm{d}\theta\,\mathrm{d}\Psi}{\pi(\cos^2\theta_{\min} - \cos^2\theta_{\max})}, \end{aligned} \tag{39}$$

where $\theta_{\min} = 0$ and $\theta_{\max} = \pi/2$ are the limit incidence angles of the plane waves composing the diffuse field.

In Eq. (39) the shell is assumed to be completely submerged in the diffuse field. The term $10\log_{10}(\pi)$ indicates that the excited surface is not just a plan projection of the shell surface (assumption used in the development of $\mathrm{TL}(\omega) = -10\log_{10}(\tau_d(\omega))$.

The maximum order n of the circumferential modes to consider in the summation of the relation (36) must be slightly higher than

$$n_{\max} = \frac{\omega}{c_0} R\sqrt{1 - \sin^2\theta\cos^2\Psi}. \tag{40}$$

This condition arises from the physical argument that the acoustic transmission considered here is a forced solution problem and thus the propagating wave number in the structure cannot be higher than the acoustic excitation wave number.

7. Numerical results and validation

The presented laminated composite model (Section 2.2) and discrete thick laminate model (Section 2.3) have been compared to Blaise et al. models for the different oblique incidence transmission loss configurations presented in their papers [5,6,13]. The results have been found identical and are not repeated here for the sake of conciseness. Instead we will limit the presentation to the validation of (i) the solution to the dispersion equations (= to the propagating wavenumbers in particular) and (ii) diffuse field transmission loss for both laminate composite and composite sandwich configurations. Table 1 gives the properties of the materials used for the different validation cases.

7.1. Dispersion curves validation

The propagative solutions of the dispersion relations (9) and (15) are presented in Figs. 4–6 for a symmetrical laminated composite made up of seven layers (0/45/-45/90/-45/45/0) of Material #2 (see Table 1). The heading direction of the propagative solutions, in Figs. 4–6 are $0^\circ, 45^\circ$ and 90°, respectively. The layers' thicknesses are: $h_{i=1\ldots7} = 0.00225\,\text{m}$. In these figures the symmetrical laminate composite model (Section 2.2) is compared to the discrete thick laminate composite model (Section 2.3). The results obtained with these two models for laminated composite cylinders are identical. At any heading direction the panel has two propagative solutions below the ring frequency. At the ring frequency a third solution becomes propagative. In the dispersion field

Table 1
Materials' properties for diffuse field transmission loss validations

	Material #1	Material #2	Material #3	Material #4	Material #5	Material #6
E_L (Pa)	2.1×10^{11}	1.25×10^{11}	0.48×10^{11}	0.1448×10^{9}	0.665×10^{6}	180×10^{9}
E_T (Pa)	2.1×10^{11}	10^{10}	0.48×10^{11}	0.1448×10^{9}	0.665×10^{6}	180×10^{9}
G_{LT} (Pa)	8.0769×10^{10}	5.9×10^{9}	0.181×10^{11}	0.5×10^{8}	0.25×10^{6}	6.767×10^{10}
G_{LZ} (Pa)	8.0769×10^{10}	3×10^{9}	0.2757×10^{10}	0.5×10^{8}	0.25×10^{6}	6.767×10^{10}
G_{TZ} (Pa)	8.0769×10^{10}	5.9×10^{9}	0.2757×10^{10}	0.5×10^{8}	0.25×10^{6}	6.767×10^{10}
v_{LT}	0.3	0.4	0.3	0.45	0.33	0.33
ρ (kg/m^3)	7800	1600	1550	110.44	2000	7720

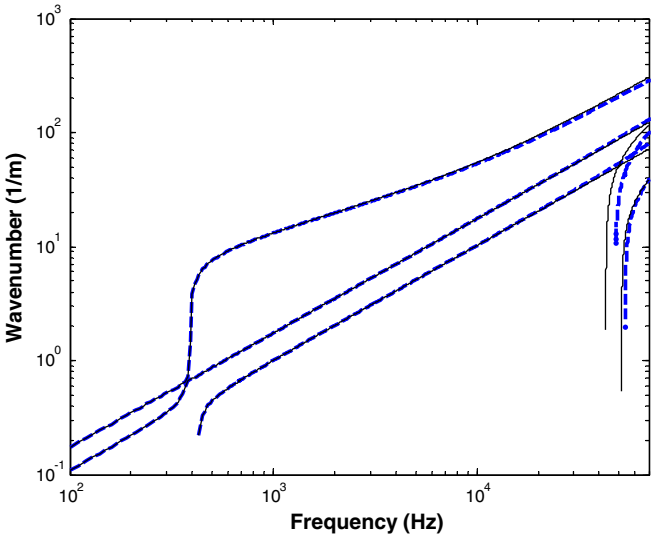

Fig. 4. Laminated composite shell's dispersion curves $\Phi = 0^\circ$: (––) discrete laminate model, (—) symmetrical laminate model.

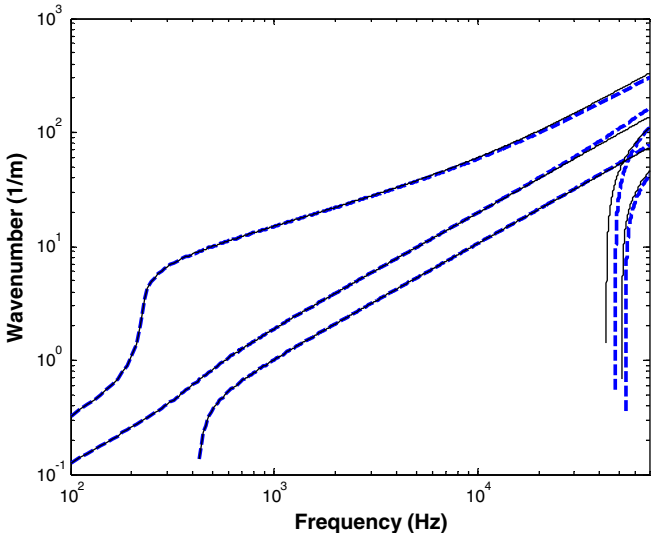

Fig. 5. Laminated composite shell's dispersion curves $\Phi = 45^\circ$: (––) discrete laminate model, (—) symmetrical laminate model.

context the ring frequency is mathematically perceived as a cut-off frequency. Two others cut-off frequencies appear at high frequencies where two additional solutions become propagative.

Next, we consider a composite sandwich and compare the presented general discrete thick laminate composite model (Section 2.3) to the sandwich model presented by Heron [8]. It is worth

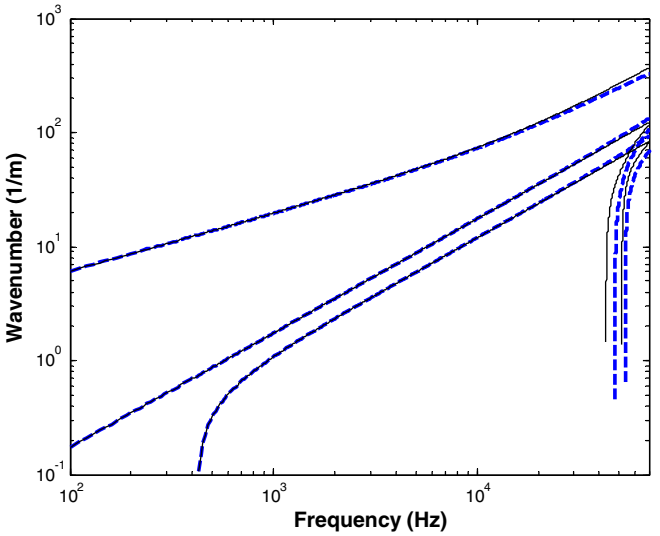

Fig. 6. Laminated composite shell's dispersion curves $\Phi = 90^\circ$: (– –) discrete laminate model, (—) symmetrical laminate model.

recalling here that Heron's model [8] is also based on a discrete approach using the classical assumptions for a laminate sandwich (e.g. thin laminate skins, a shear bearing core). It leads to a 47 order dispersion system. On the other hand, the presented discrete thick laminate model assumes all layers (skins and core) to be laminate and thick and lead to a 42 order dispersion system. The skins of the studied cylinder are made up from Material #3 and the core from Material #4. The layers' thicknesses are: $h_1 = h_2 = 0.0012$ and $h_3 = 0.0127$ m. The propagating wavenumbers are presented in Figs. 7–9 for a heading direction of $0^\circ, 45^\circ$ and 90°, respectively. It is observed that for this thin skin sandwich, the two models lead to identical solutions. In consequence, the presented discrete laminate models can handle accurately both laminate composites and sandwich composite shells.

Note that in the proposed discrete laminate model, full composite behaviours are considered in each layer in order to handle various real-life configurations. In several sandwich/laminate structures, distinct layers are not always governed by pure bending behaviours (e.g. skin in sandwich theory) or shear (e.g. core in sandwich theory). A typical example is a tri-layers structure made up from a core with two viscoelastic skins (symmetric free layer damping treatment). Here, the core works in bending while the skins are working in traction/compression. Classical assumptions of the sandwich theory will not, justly enough, correctly model this configuration. Another example concerns a tri-layers structure with limp skins. The following case is considered numerically. The structure has 1 mm skins made up from Material #5 and 3 mm core of Material #6. The dispersion curves computed using the present discrete laminate theory and the sandwich shell theory are given in Fig. 10. It is clearly observed that classical sandwich assumptions completely miss the physics of the problem.

Another example showing the generality and versatility of the proposed general discrete layer approach compared to the classical sandwich theory is the case of a sandwich structure made up

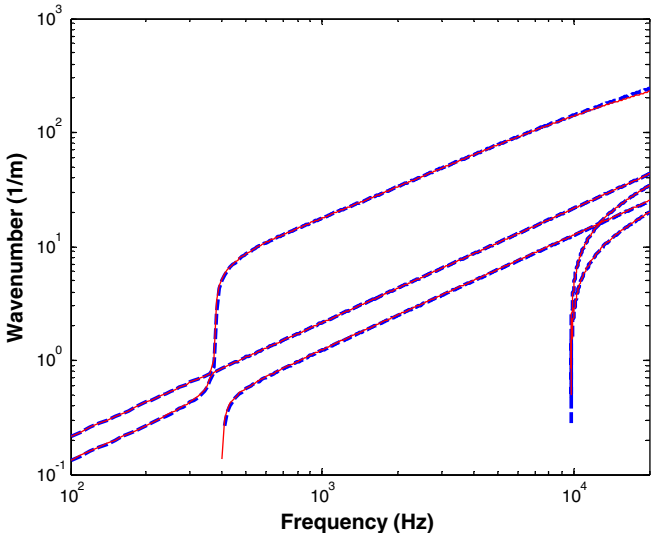

Fig. 7. Laminated composite sandwich shell's dispersion curves $\Phi = 0^{\circ}$: (−−) discrete laminate model, (—) sandwich laminate model by Heron [8].

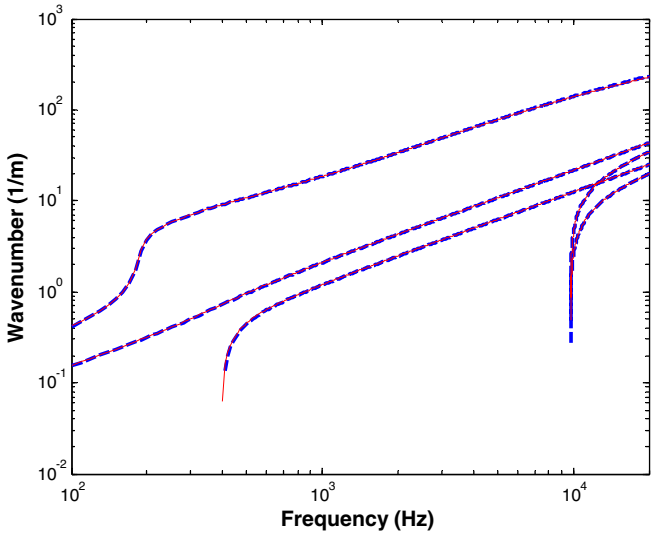

Fig. 8. Laminated composite sandwich shell's dispersion curves $\Phi = 45^{\circ}$: (− −) discrete laminate model, (—) sandwich laminate model by Heron [8].

from a shear core and two thick skins. The studied structure is made up from 2.5 cm thick skins of Material #3 and a 1 cm thick core of Material #4. The dispersion curves obtained using the proposed discrete theory and the sandwich shell theories are given in Fig. 11. To better visualize the asymptotical tendencies in mid-to-high frequencies, the skins dispersion curves are also represented using thick and thin plate theories. It is clearly seen that at mid-and-high frequencies the sandwich theory is not able to correctly capture the shear effects in the skins.

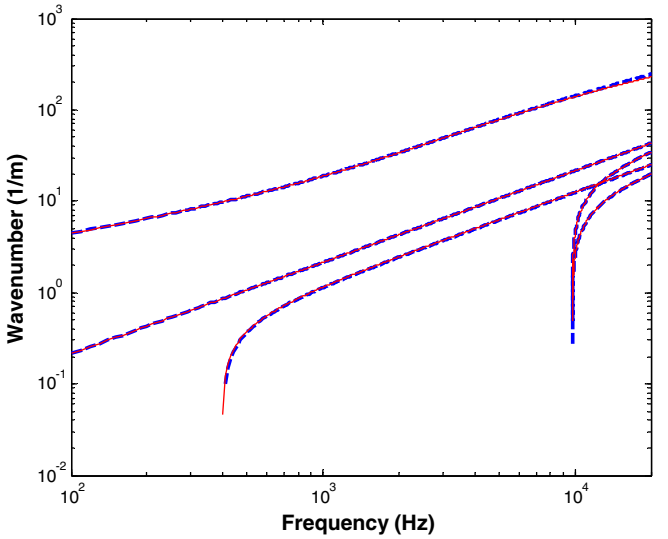

Fig. 9. Laminated composite sandwich shell's dispersion curves $\Phi = 90°$: (– –) discrete laminate model, (—) sandwich laminate model by Heron [8].

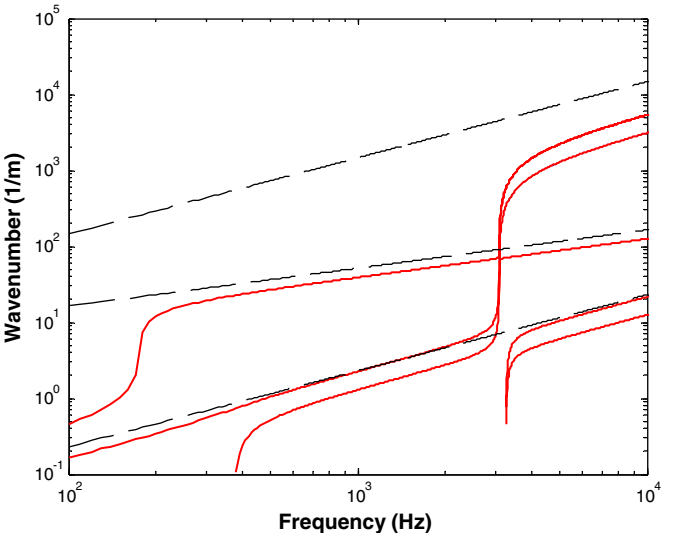

Fig. 10. Limp skins sandwich composite shell's dispersion curves $\Phi = 45°$: (—) discrete laminate model, (– –) sandwich laminate model by Heron [8].

7.2. *Diffuse field transmission loss validations*

First, we consider a cylinder (Material #1) having a thickness $h = 3$ mm. The curvature radius of the cylinder is 2 m and the structural loss factor of all layers is 0.001. The layers continuity

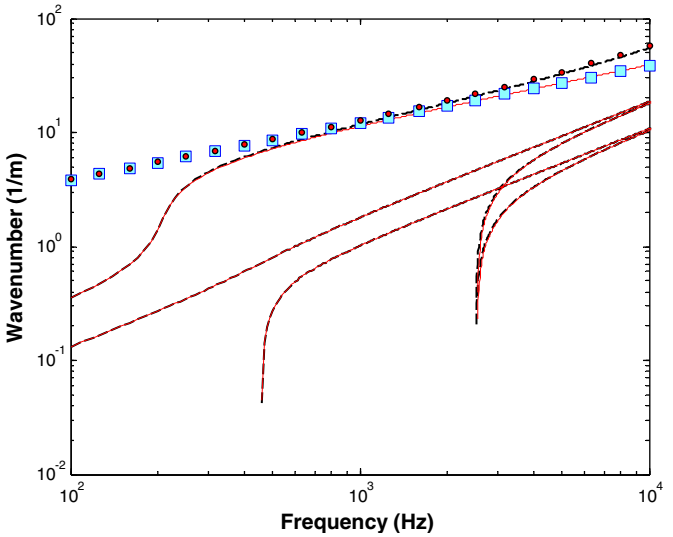

Fig. 11. Thick skins sandwich composite shell's dispersion curves $\Phi = 45^\circ$: (– –) discrete laminate model, (—) sandwich laminate model by Heron [8], (○ ○ ○) skin alone (thick plate theory) (□ □ □) skin alone (thin plate theory).

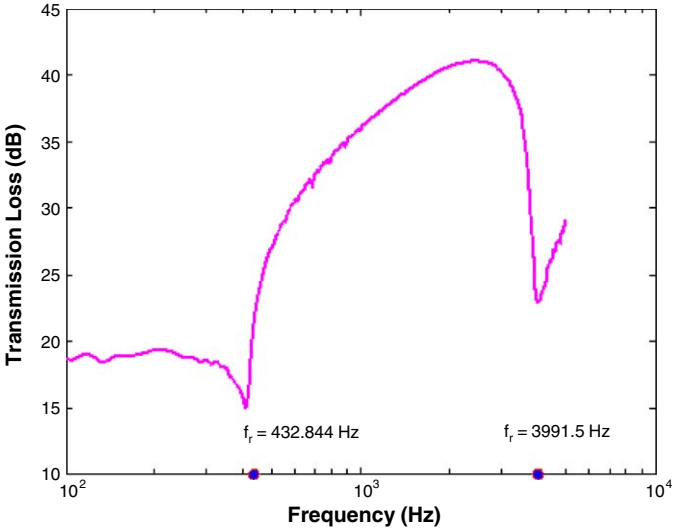

Fig. 12. Interlayer continuity conditions validation. Ring frequency and critical frequencies relations validation for laminated isotropic shell (Material #1); (—) one layer and (—) three layers simulations.

conditions and the numerical implementation of the relations (19) and (25) for the laminated shell are verified by comparing the diffuse field transmission loss of the single layer shell to the same shell artificially subdivided into three identical layers ($h_1 = h_2 = h_3 = 1$ mm). The results are given in Fig. 12. A total agreement is found between the two configurations. Moreover, in order to

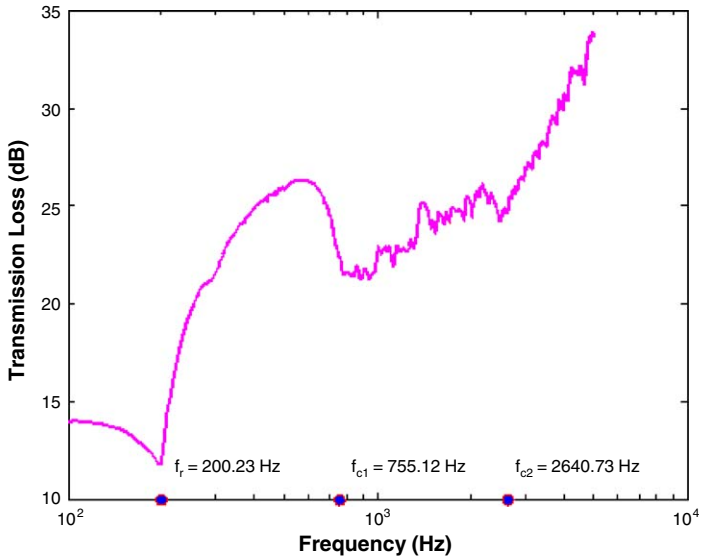

Fig. 13. Interlayer continuity conditions validation. Ring frequency and critical frequencies relations validation for laminated composite shell (Material #2); (—) one layer and (—) five layers simulations.

validate the relations of the critical frequencies and the ring frequency, the minima of the transmission loss estimations are compared to the values of the ring and critical frequencies calculated by relations (19) and (25). These computed values are added in Fig. 12. It can be observed that they are accurately estimated. The same validation is considered in Fig. 13 for an orthotropic cylinder made up from Material #2 (Graphite epoxy). Two configurations are considered: single layer with a total thickness $h = 10\,\text{mm}$ and a five layers shell of the same material and thickness ($h_1 = \cdots = h_5 = 2\,\text{mm}$). Once again, the estimations of the ring frequency and critical frequencies are excellent.

The diffuse field transmission loss of a symmetrical laminate composite cylinder is presented in Fig. 14. The curvature radius of the cylinders considered is 2 m. The cylinder is made up of seven layers (0/45/-45/90/-45/45/0) of Material #2 (see Table 1) and the thicknesses of the layers are $h_{i=1\ldots7} = 0.00125$. The structural loss factor of all layers is 0.01. In this figure the symmetrical laminate composite model (Section 2.2) is compared to the discrete thick laminate composite model (Section 2.3). Once again, the results obtained with these two models for laminated composite cylinders are identical. The ring and critical frequencies of the laminated composite cylinder are numerically estimated and shown in Fig. 14: $f_r = 422.24\,\text{Hz}$; $f_{c1} = 981.96\,\text{Hz}$; $f_{c2} = 2083.5244\,\text{Hz}$.

Next, the discrete laminate composite model (Section 2.3) is compared in Fig. 15 with the Heron' model [8] for the sandwich composite cylinder studied in the previous section. Once again it is observed that these two models lead to identical solutions. The computed values of the ring frequency and the critical frequency are shown in Fig. 15; $f_r = 401.8\,\text{Hz}$; $f_c = 1134.1\,\text{Hz}$. An excellent agreement is observed between the ring and critical frequencies locus in the transmission loss results and the direct computed values.

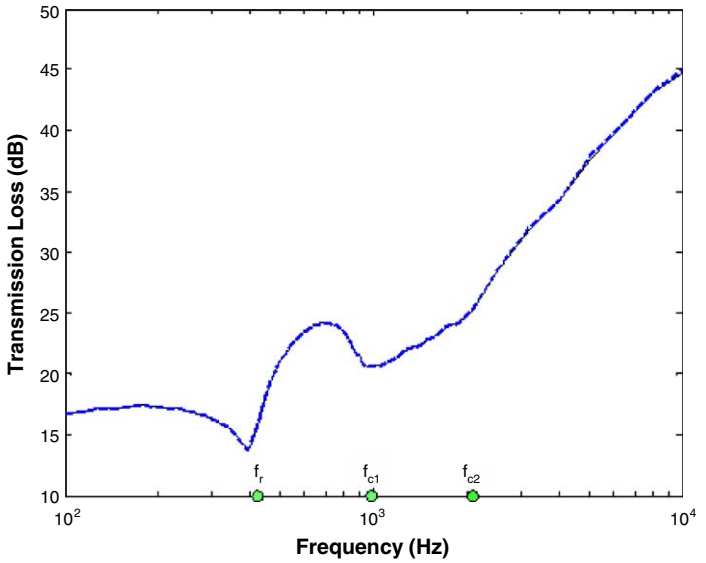

Fig. 14. Laminated composite cylinder modelling; (––) symmetrical laminate and (—) discrete laminate simulations.

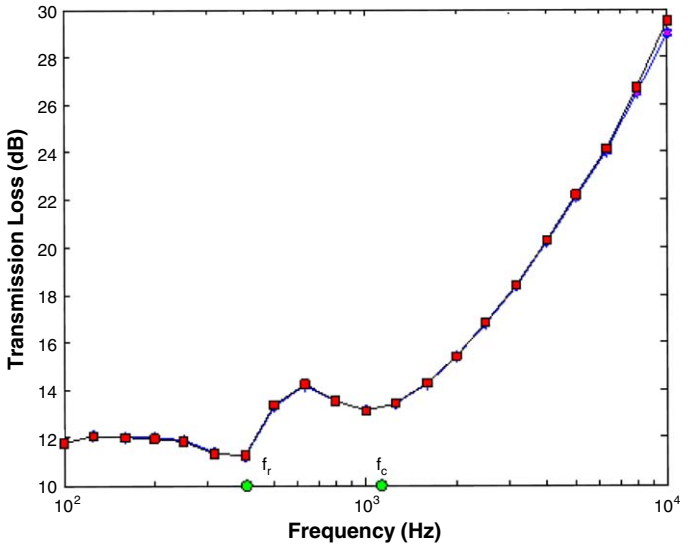

Fig. 15. Laminated composite sandwich cylinders modelling; (–⋆–) discrete laminate and (–■–) sandwich laminate [8] simulations.

8. Experimental validation

Finally an experimental validation of the proposed formulation is proposed. It consists of the transmission loss of a curved finite sandwich composite panel. The panel has side dimensions $1.37 \times 1.65\,m^2$, a 2 m radius, 0.0014732 m thick skins made up of Material #3 and 0.0127 m thick core made up of Material #4. The tests are done at the reverberant-anechoic facility of GAUS

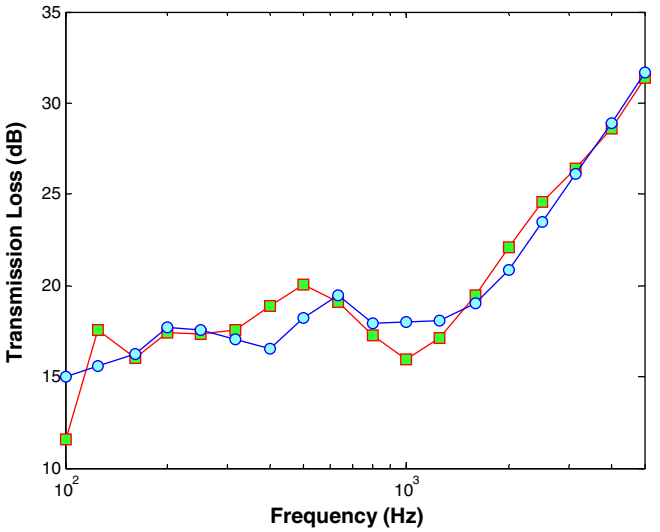

Fig. 16. Finite curved sandwich composite panel—experimental validation: (–■–) experimental; (–•–) numerical simulation.

(Groupe Acoustique de l'Université de Sherbrooke). Great care was taken to install the panel to eliminate leaks and minimize the damping effects of the mounting. The results are given in Fig. 16. The numerical result is obtained using a statistical energy analysis scheme using a wavenumber approach based on the proposed discrete laminate theory. Details of the calculations of the necessary parameters (modal density, radiation efficiency, non-resonant transmission and resonant transmission) for the SEA calculations can be found in Ref. [14]. The damping loss factor was taken constant by band with values from 1% to 2.5%. Still, excellent agreement is observed between numerical simulation and experiment. In particular, the model is able to correctly capture the ring and critical frequency regions. Better agreement can be found using an experimentally measured damping loss factor.

9. Conclusions

The paper discusses the modelling of the diffuse field transmission loss through infinite laminated composite cylindrical cylinders. Two models were presented and compared; the first is limited to symmetrically laminate composite shells and the second is more general and is based on a discrete layer theory. For each model, membrane, bending, transverse shearing as well as rotational inertia effects and orthotropic ply angle of the layers are considered. Moreover in the symmetrically laminate composite model, the accurate estimation of the shear correction coefficients is crucial. Expressions for the numerical calculation of the structural impedance, the critical frequencies and the ring frequency were also given in both cases. The two models were compared for symmetrical laminate composite cylinders and found similar. Moreover, for sandwich configurations, the discrete layer model was compared successfully to Heron' sandwich

composite model [8]. Finally, the discrete laminate composite model was successfully compared with experimental results in the case of a finite sandwich curved panel.

In conclusion, it is suggested that the presented discrete model is an appropriate general model. It allows for both symmetrical and asymmetrical laminated composite and/or sandwich-type composite panels with thin or thick laminate skins. Moreover, its computational cost is acceptable (42 eigenvalue system compared to 10 for the thick laminate or 47 for the Heron's sandwich model).

Appendix A. Main equations of the laminate composite model

A.1. Equilibrium equations

The resultant stress forces and moments of the laminate are defined as in Ref. [9]

$$Q_x = \int_{-h/2}^{h/2} \tau_{xz}\left(1+\frac{z}{R}\right) dz = \sum_{k=1}^{N} \int_{h_{lk}}^{h_{uk}} \tau_{xz}^{k}\left(1+\frac{z}{R}\right) dz,$$

$$Q_y = \int_{-h/2}^{h/2} \tau_{yz}\, dz = \sum_{k=1}^{N} \int_{h_{lk}}^{h_{uk}} \tau_{yz}^{k}\, dz, \tag{A.1}$$

$$N_x = \int_{-h/2}^{h/2} \sigma_x\left(1+\frac{z}{R}\right) dz = \sum_{k=1}^{N} \int_{h_{lk}}^{h_{uk}} \sigma_x^{k}\left(1+\frac{z}{R}\right) dz,$$

$$N_y = \int_{-h/2}^{h/2} \sigma_y\, dz = \sum_{k=1}^{N} \int_{h_{lk}}^{h_{uk}} \sigma_y^{k}\, dz,$$

$$N_{xy} = \int_{-h/2}^{h/2} \tau_{xy}\left(1+\frac{z}{R}\right) dz = \sum_{k=1}^{N} \int_{h_{lk}}^{h_{uk}} \tau_{xy}^{k}\left(1+\frac{z}{R}\right) dz,$$

$$N_{yx} = \int_{-h/2}^{h/2} \tau_{yx}\, dz = \sum_{k=1}^{N} \int_{h_{lk}}^{h_{uk}} \tau_{yx}^{k}\, dz,$$

$$M_x = \int_{-h/2}^{h/2} \sigma_x z\left(1+\frac{z}{R}\right) dz = \sum_{k=1}^{N} \int_{h_{lk}}^{h_{uk}} \sigma_x^{k} z\left(1+\frac{z}{R}\right) dz,$$

$$M_y = \int_{-h/2}^{h/2} \sigma_y z\, dz = \sum_{k=1}^{N} \int_{h_{lk}}^{h_{uk}} \sigma_y^{k} z\, dz,$$

$$M_{xy} = \int_{-h/2}^{h/2} \tau_{xy} z\left(1+\frac{z}{R}\right) dz = \sum_{k=1}^{N} \int_{h_{lk}}^{h_{uk}} \tau_{xy}^{k} z\left(1+\frac{z}{R}\right) dz,$$

$$M_{yx} = \int_{-h/2}^{h/2} \tau_{yx} z\, dz = \sum_{k=1}^{N} \int_{h_{lk}}^{h_{uk}} \tau_{yx}^{k} z\, dz. \tag{A.2}$$

Using the notations presented in Figs. 1a and 2, the integral limits h_{uk} and h_{lk} in the relations (A.1) and (A.2) are computed using the following relations:

$$h_{uk} = \frac{h}{2} - \sum_{j=0}^{k-1} h_j, \quad h_{lk} = \frac{h}{2} - \sum_{j=1}^{k} h_j, \tag{A.3}$$

where h is the total thickness of the shell and h_j is the thickness of lamina j (for $j = 0, h_j = h_0 = 0$).

The transverse shear-stress forces used in equilibrium equations (3) are defined as follows:

$$\begin{aligned} Q_x &= F_{45}\left(w_{,y} + \varphi_y - \frac{v}{R}\right) + F_{55}(w_{,x} + \varphi_x) + H_{55}\left(\frac{w_{,x}}{R} + \frac{\varphi_x}{R}\right), \\ Q_y &= F_{44}\left(w_{,y} + \varphi_y - \frac{v}{R}\right) + F_{45}(w_{,x} + \varphi_x) + H_{44}\left(\frac{v}{R^2} - \frac{\varphi_y}{R} - \frac{w_{,y}}{R}\right) \end{aligned} \tag{A.4}$$

and the in-plane stress forces

$$\begin{aligned} N_x = {} & A_{11}u_{,x} + A_{12}\left(v_{,y} + \frac{w}{R}\right) + A_{16}(u_{,y} + v_{,x}) + B_{11}\left(\frac{u_{,x}}{R} + \varphi_{x,x}\right) \\ & + \cdots + B_{12}\varphi_{y,y} + B_{16}\left(\frac{v_{,x}}{R} + \varphi_{x,y} + \varphi_{y,x}\right) + D_{11}\frac{\varphi_{x,x}}{R} + D_{16}\frac{\varphi_{y,x}}{R}, \end{aligned}$$

$$\begin{aligned} N_{xy} = {} & A_{16}u_{,x} + A_{26}\left(v_{,y} + \frac{w}{R}\right) + A_{66}(u_{,y} + v_{,x}) + B_{16}\left(\frac{u_{,x}}{R} + \varphi_{x,x}\right) \\ & + \cdots + B_{26}\varphi_{y,y} + B_{66}\left(\frac{v_{,x}}{R} + \varphi_{x,y} + \varphi_{y,x}\right) + D_{16}\frac{\varphi_{x,x}}{R} + D_{66}\frac{\varphi_{y,x}}{R}, \end{aligned}$$

$$\begin{aligned} N_y = {} & A_{12}u_{,x} + A_{22}\left(v_{,y} + \frac{w}{R}\right) + A_{26}(u_{,y} + v_{,x}) + B_{12}\varphi_{x,x} \\ & + \cdots + B_{22}\left(\varphi_{y,y} - \frac{v_{,y}}{R} - \frac{w}{R^2}\right) + B_{26}\left(\varphi_{x,y} + \varphi_{y,x} - \frac{u_{,y}}{R}\right) \\ & - D_{22}\frac{\varphi_{y,y}}{R} - D_{26}\frac{\varphi_{x,y}}{R}, \end{aligned}$$

$$\begin{aligned} N_{yx} = {} & A_{16}u_{,x} + A_{26}\left(v_{,y} + \frac{w}{R}\right) + A_{66}(u_{,y} + v_{,x}) + B_{16}\varphi_{x,x} \\ & + \cdots + B_{26}\left(\varphi_{y,y} - \frac{v_{,y}}{R} - \frac{w}{R^2}\right) + B_{66}\left(\varphi_{x,y} + \varphi_{y,x} - \frac{u_{,y}}{R}\right) \\ & - D_{26}\frac{\varphi_{y,y}}{R} - D_{66}\frac{\varphi_{x,y}}{R} \end{aligned} \tag{A.5}$$

as well as the stress moments

$$\begin{aligned} M_x = {} & B_{11}u_{,x} + B_{12}\left(v_{,y} + \frac{w}{R}\right) + B_{16}(u_{,y} + v_{,x}) + D_{11}\left(\frac{u_{,x}}{R} + \varphi_{x,x}\right) \\ & + \cdots + D_{12}\varphi_{y,y} + D_{16}\left(\frac{v_{,x}}{R} + \varphi_{x,y} + \varphi_{y,x}\right), \end{aligned}$$

$$M_y = B_{12}u_{,x} + B_{22}\left(v_{,y} + \frac{w}{R}\right) + B_{26}(u_{,y} + v_{,x}) + D_{12}\varphi_{x,x} + \cdots + D_{22}\left(\varphi_{y,y} - \frac{v_{,y}}{R} - \frac{w}{R^2}\right) + D_{26}\left(\varphi_{x,y} + \varphi_{y,x} - \frac{u_{,y}}{R}\right),$$

$$M_{xy} = B_{16}u_{,x} + B_{26}\left(v_{,y} + \frac{w}{R}\right) + B_{66}(u_{,y} + v_{,x}) + D_{16}\left(\frac{u_{,x}}{R} + \varphi_{x,x}\right) + \cdots + D_{26}\varphi_{y,y} + D_{66}\left(\frac{v_{,x}}{R} + \varphi_{x,y} + \varphi_{y,x}\right),$$

$$M_{yx} = B_{16}u_{,x} + B_{26}\left(v_{,y} + \frac{w}{R}\right) + B_{66}(u_{,y} + v_{,x}) + D_{16}\varphi_{x,x} + \cdots + D_{26}\left(\varphi_{y,y} - \frac{v_{,y}}{R} - \frac{w}{R^2}\right) + D_{66}\left(\varphi_{x,y} + \varphi_{y,x} - \frac{u_{,y}}{R}\right). \tag{A.6}$$

The inertial terms in the equilibrium equations (3) are expressed by the following relations:

$$m_s = \sum_{k=1}^{N} [\rho_k(h_{uk} - h_{lk})],$$
$$I_z = \sum_{k=1}^{N} \left[\rho_k \frac{(h_{uk}^3 - h_{lk}^3)}{3}\right],$$
$$I_{z2} = \sum_{k=1}^{N} \left[\rho_k \frac{(h_{uk}^2 - h_{lk}^2)}{2}\right], \tag{A.7}$$

where m_s is the mass per unit area, I_z is the rotational inertia and ρ_k is the mass density of the layer k. The elastic constants derived in (A.4)–(A.6) are defined by the following relations:

$$\left.\begin{aligned} A_{ij} &= \sum_{k=1}^{N} Q_{ij}^k(h_{uk} - h_{lk}),\\ B_{ij} &= \sum_{k=1}^{N} Q_{ij}^k \frac{h_{uk}^2 - h_{lk}^2}{2},\\ D_{ij} &= \sum_{k=1}^{N} Q_{ij}^k \frac{h_{uk}^3 - h_{lk}^3}{3},\\ F_{ij} &= \kappa_{ij} \sum_{k=1}^{N} C_{ij}^k(h_{uk} - h_{lk}),\\ H_{ij} &= \kappa_{ij} \sum_{k=1}^{N} C_{ij}^k \frac{h_{uk}^2 - h_{lk}^2}{2}, \end{aligned}\right\} \; i,j = 4;5, \tag{A.8a}$$

$$
\left.
\begin{aligned}
A^*_{ij} &= \sum_{k=1}^{N} Q^k_{ij}(h_{uk} - h_{lk})(1 + i\eta_k),\\
B^*_{ij} &= \sum_{k=1}^{N} Q^k_{ij}\,\frac{h^2_{uk} - h^2_{lk}}{2}(1 + i\eta_k),\\
D^*_{ij} &= \sum_{k=1}^{N} Q^k_{ij}\,\frac{h^3_{uk} - h^3_{lk}}{3}(1 + i\eta_k)\\
F^*_{ij} &= \kappa_{ij}\sum_{k=1}^{N} C^k_{ij}(h_{uk} - h_{lk})(1 + i\eta_k),\\
H^*_{ij} &= \kappa_{ij}\sum_{k=1}^{N} C^k_{ij}\,\frac{h^2_{uk} - h^2_{lk}}{2}(1 + i\eta_k),
\end{aligned}
\right\} \quad i,j = 4;5 \tag{A.8b}
$$

where κ_{ij} are the transverse shear correction factors [15], $i = \sqrt{-1}, \eta_k$ is the k layer's structural damping coefficient and Q^k_{ij} are the k layer's in-plane elastic constants defined by the following relations as shown by Berthelot [10]

$$
\begin{aligned}
Q^k_{11} &= C^k_L \cos^4\theta_k + C^k_T \sin^4\theta_k + 2(C^k_{LT} + 2G^k_{LT})\sin^2\theta_k \cos^2\theta_k,\\
Q^k_{12} &= (C^k_L + C^k_T - 4G^k_{LT})\sin^2\theta_k \cos^2\theta_k + C^k_{LT}(\cos^4\theta_k + \sin^4\theta_k),\\
Q^k_{16} &= (C^k_L - C^k_{LT} - 2G^k_{LT})\ \sin\theta_k \cos^3\theta_k\\
&\quad + (C^k_{LT} - C^k_T + 2G^k_{LT})\sin^3\theta_k \cos\theta_k,\\
Q^k_{22} &= C^k_L \sin^4\theta_k + C^k_T \cos^4\theta_k + 2(C^k_{LT} + 2G^k_{LT})\sin^2\theta_k \cos^2\theta_k,\\
Q^k_{26} &= (C^k_L - C^k_{LT} - 2G^k_{LT})\sin^3\theta_k\ \cos\theta_k\\
&\quad + (C^k_{LT} - C^k_T + 2G^k_{LT})\sin\theta_k \cos^3\theta_k,\\
Q^k_{66} &= (C^k_L + C^k_T - 2(C^k_{LT} + G^k_{LT}))\sin^2\theta_k \cos^2\theta_k\\
&\quad + G^k_{LT}(\cos^4\theta_k + \sin^4\theta_k),
\end{aligned} \tag{A.9}
$$

$$
C^k_L = \left(\frac{E^k_L}{1 - \nu^k_{LT}\nu^k_{TL}}\right) \quad C^k_T = \left(\frac{E^k_T}{1 - \nu^k_{LT}\nu^k_{TL}}\right) \quad C^k_{LT} = \left(\frac{\nu^k_{LT}E^k_{LT}}{1 - \nu^k_{LT}\nu^k_{TL}}\right) \tag{A.10}
$$

and C^k_{ij} are the k layer's transversal shear elastic constants are defined as [10]

$$
\begin{aligned}
C^k_{44} &= G^k_{TZ}\cos^2\theta_k + G^k_{LZ}\sin^2\theta_k,\\
C^k_{45} &= (G^k_{LZ} - G^k_{TZ})\sin\theta_k + \cos\theta_k,\\
C^k_{55} &= G^k_{LZ}\cos^2\theta_k + G^k_{TZ}\sin^2\theta_k.
\end{aligned} \tag{A.11}
$$

There are several methods for computing the shear correction coefficients. The models of Berthelot [10], Guy [16] and Batoz et al. [15] for transversal shear coefficients computation were tested and found identical. The approach presented in Batoz [15] is selected for its simplicity.

The elastic coefficients in Eqs. (A.9) and (A.11) are represented according to the orthotropic angles θ_k shown in Fig. 17 as the angles between the principal coordinate system of each layer $k(L\text{-}0\text{-}T)$ and the global coordinate system of the shell (x-0-y).

The dynamic equilibrium equations of the shell are rewritten, after appropriate algebraic manipulations as

$$\left(A_{11}+\frac{B_{11}}{R}\right)u_{,xx}+2A_{16}u_{,xy}+\left(A_{66}-\frac{B_{66}}{R}\right)u_{,yy}+\left(A_{16}+\frac{B_{16}}{R}\right)v_{,xx}$$
$$+(A_{12}+A_{66})v_{,xy}+\left(A_{26}-\frac{B_{26}}{R}\right)v_{,yy}+\left(B_{11}+\frac{D_{11}}{R}\right)\varphi_{x,xx}+2B_{16}\varphi_{x,xy}$$
$$+\left(B_{66}-\frac{D_{66}}{R}\right)\varphi_{x,yy}+\left(B_{16}+\frac{D_{16}}{R}\right)\varphi_{y,xx}+(B_{12}+B_{66})\varphi_{y,xy}+\left(B_{26}-\frac{D_{26}}{R}\right)\varphi_{y,yy}$$
$$+\frac{A_{12}}{R}w_{,x}+\left(\frac{A_{26}}{R}-\frac{B_{26}}{R^2}\right)w_{,y}+\left(m_s u+\frac{I_z}{R}\varphi_x\right)\omega^2=0,$$

$$\left(A_{16}+\frac{B_{16}}{R}\right)u_{,xx}+(A_{12}+A_{66})u_{,xy}+\left(A_{26}-\frac{B_{26}}{R}\right)u_{,yy}$$
$$+\left(A_{66}+\frac{B_{66}}{R}\right)v_{,xx}+2A_{26}v_{,xy}+\left(A_{22}-\frac{B_{22}}{R}\right)v_{,yy}+\left(B_{16}+\frac{D_{16}}{R}\right)\varphi_{x,xx}$$
$$+(B_{12}+B_{66})\varphi_{x,xy}+\left(B_{26}-\frac{D_{26}}{R}\right)\varphi_{x,yy}+\left(B_{66}+\frac{D_{66}}{R}\right)\varphi_{y,xx}$$
$$+2B_{26}\varphi_{y,xy}+\left(B_{22}-\frac{D_{22}}{R}\right)\varphi_{y,yy}+\left(\frac{A_{26}}{R}+\frac{F_{45}}{R}\right)w_{,x}$$
$$+\left(\frac{A_{22}}{R}-\frac{B_{22}}{R^2}+\frac{F_{44}}{R}-\frac{H_{44}}{R^2}\right)w_{,y}-\left(\frac{F_{44}}{R^2}-\frac{H_{44}}{R^3}\right)v+\frac{F_{45}}{R}\varphi_x$$
$$+\left(\frac{F_{44}}{R}-\frac{H_{44}}{R^2}\right)\varphi_y+\left(m_s v+\frac{I_z}{R}\varphi_y\right)\omega^2=0,$$

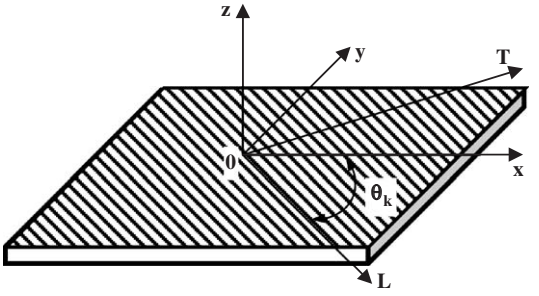

Fig. 17. Orthotropic directions of a layer.

$$
\begin{aligned}
&\left(F_{55}+\frac{H_{55}}{R}\right)w_{,xx}+2F_{45}w_{,xy}+\left(F_{44}-\frac{H_{44}}{R}\right)w_{,yy}-\frac{A_{12}}{R}\,u_{,x}\\
&-\left(\frac{A_{26}}{R}-\frac{B_{26}}{R^2}\right)u_{,y}-\left(\frac{A_{26}}{R}+\frac{F_{45}}{R}\right)v_{,x}-\left(\frac{A_{22}}{R}-\frac{B_{22}}{R^2}+\frac{F_{44}}{R}-\frac{H_{44}}{R^2}\right)v_{,y}\\
&-\left(\frac{B_{12}}{R}-F_{55}-\frac{H_{55}}{R}\right)\varphi_{x,x}-\left(\frac{B_{26}}{R}-\frac{D_{26}}{R^2}-F_{45}\right)\varphi_{x,y}\\
&-\left(\frac{B_{26}}{R}-F_{45}\right)\varphi_{y,x}-\left(\frac{B_{22}}{R}-\frac{D_{22}}{R^2}-F_{44}+\frac{H_{44}}{R}\right)\varphi_{y,y}\\
&-\left(\frac{A_{22}}{R}-\frac{B_{22}}{R^3}\right)w+m_s\omega^2 w=0,
\end{aligned}
$$

$$
\begin{aligned}
&\left(B_{11}+\frac{D_{11}}{R}\right)u_{,xx}+2B_{16}u_{,xy}+\left(B_{66}-\frac{D_{66}}{R}\right)u_{,yy}\\
&+\left(B_{16}+\frac{D_{16}}{R}\right)v_{,xx}+(B_{12}+B_{66})v_{,xy}\left(B_{26}-\frac{D_{26}}{R}\right)v_{,yy}+D_{11}\varphi_{x,xx}\\
&+2D_{16}\varphi_{x,xy}+D_{66}\varphi_{x,yy}+D_{16}\varphi_{y,xx}+(D_{12}+D_{66})\varphi_{y,xy}+D_{26}\varphi_{y,yy}\\
&+\left(\frac{B_{12}}{R}-F_{55}-\frac{H_{55}}{R}\right)w_{,x}+\left(\frac{B_{26}}{R}-\frac{D_{26}}{R^2}-F_{45}\right)w_{,y}\\
&+\frac{F_{45}}{R}\,v-\left(F_{55}+\frac{H_{55}}{R}\right)\varphi_x-F_{45}\varphi_y+I_z\omega^2\left(\varphi_x+\frac{u}{R}\right)=0,
\end{aligned}
$$

$$
\begin{aligned}
&\left(B_{16}+\frac{D_{16}}{R}\right)u_{,xx}+(B_{12}+B_{66})u_{,xy}+\left(B_{26}-\frac{D_{26}}{R}\right)u_{,yy}\\
&+\left(B_{66}+\frac{D_{66}}{R}\right)v_{,xx}+2B_{26}v_{,xy}+\left(B_{22}-\frac{D_{22}}{R}\right)v_{,yy}\\
&+D_{16}\varphi_{x,xx}+(D_{12}+D_{66})\varphi_{x,xy}\\
&+D_{26}\varphi_{x,yy}+D_{66}\varphi_{y,xx}+2D_{26}\varphi_{y,xy}+D_{22}\varphi_{y,yy}+\left(\frac{B_{26}}{R}-F_{45}\right)w_{,x}\\
&-\left(\frac{B_{22}}{R}-\frac{D_{22}}{R^2}-F_{44}+\frac{H_{44}}{R}\right)w_{,y}+\left(\frac{F_{44}}{R}-\frac{H_{44}}{R^2}\right)v\\
&-F_{45}\varphi_x-\left(F_{44}-\frac{H_{44}}{R}\right)\varphi_y+I_z\omega^2\left(\varphi_y+\frac{v}{R}\right)=0.
\end{aligned}
\tag{A.12}
$$

A.2. Dispersion system matrices

The matrices $[A_0]$, $[A_1]$, $[A_2]$ used in Eq. (7) are defined as follows:

$$[A_0] = \begin{bmatrix} m_s\omega^2 & 0 & 0 & I_z\omega^2 & 0 \\ 0 & m_s\omega^2 - \frac{F_{44}}{R^2} + \frac{H_{44}}{R^3} & 0 & \frac{F_{45}}{R} & \frac{F_{44}}{R} - \frac{H_{44}}{R^2} + \frac{I_z}{R}\omega^2 \\ 0 & 0 & m_s\omega^2 - \frac{A_{22}}{R^2} + \frac{B_{22}}{R^3} & 0 & 0 \\ \frac{I_z}{R}\omega^2 & \frac{F_{45}}{R} & 0 & I_z\omega^2 - F_{55} - \frac{H_{55}}{R} & -F_{45} \\ 0 & \frac{F_{44}}{R} - \frac{H_{44}}{R^2} + \frac{I_z}{R}\omega^2 & 0 & -F_{45} & I_z\omega^2 - F_{44} - \frac{H_{44}}{R} \end{bmatrix}$$

$$[A_1] = \begin{bmatrix} 0 & 0 & \alpha_{13} & 0 & 0 \\ 0 & 0 & \alpha_{23} & 0 & 0 \\ -\alpha_{13} & -\alpha_{23} & 0 & \alpha_{34} & \alpha_{35} \\ 0 & 0 & -\alpha_{34} & 0 & 0 \\ 0 & 0 & -\alpha_{35} & 0 & 0 \end{bmatrix}, \quad [A_2] = \begin{bmatrix} \beta_{11} & \beta_{12} & 0 & \beta_{14} & \beta_{15} \\ \beta_{12} & \beta_{22} & 0 & \beta_{24} & \beta_{25} \\ 0 & 0 & \beta_{33} & 0 & 0 \\ \beta_{14} & \beta_{24} & 0 & \beta_{44} & \beta_{45} \\ \beta_{15} & \beta_{25} & 0 & \beta_{45} & \beta_{55} \end{bmatrix} \tag{A.13}$$

with coefficients α_{ij} and β_{ij} defined as follows:

$$\begin{aligned} \alpha_{13} &= -\frac{A_{12}}{R}\cos\varphi - \left(\frac{A_{26}}{R} - \frac{B_{26}}{R^2}\right)\sin\varphi, \\ \alpha_{23} &= -\left(\frac{A_{22}}{R} - \frac{B_{22}}{R^2} + \frac{F_{44}}{R} - \frac{H_{44}}{R^2}\right)\sin\varphi - \left(\frac{A_{26}}{R} + \frac{F_{45}}{R}\right)\cos\varphi, \\ \alpha_{34} &= \left(\frac{B_{12}}{R} - F_{55} - \frac{H_{55}}{R}\right)\cos\varphi + \left(\frac{B_{26}}{R} - \frac{D_{26}}{R^2} - F_{45}\right)\sin\varphi, \\ \alpha_{35} &= \left(\frac{B_{22}}{R} - \frac{D_{22}}{R^2} - F_{44} + \frac{H_{44}}{R}\right)\sin\varphi + \left(\frac{B_{26}}{R} - F_{45}\right)\cos\varphi. \end{aligned} \tag{A.14}$$

$$\begin{aligned} \beta_{11} &= \left(A_{11} + \frac{B_{11}}{R}\right)\cos^2\varphi + 2A_{16}\cos\varphi\sin\varphi + \left(A_{66} - \frac{B_{66}}{R}\right)\sin^2\varphi, \\ \beta_{12} &= \left(A_{16} + \frac{B_{16}}{R}\right)\cos^2\varphi + (A_{12} + A_{66})\cos\varphi\sin\varphi + \left(A_{26} - \frac{B_{26}}{R}\right)\sin^2\varphi, \\ \beta_{14} &= \left(B_{11} + \frac{D_{11}}{R}\right)\cos^2\varphi + 2B_{16}\cos\varphi\sin\varphi + \left(B_{66} - \frac{D_{66}}{R}\right)\sin^2\varphi, \end{aligned}$$

$$\beta_{15} = \left(B_{16} + \frac{D_{16}}{R}\right)\cos^2\varphi + (B_{12} + B_{66})\cos\varphi\,\sin\varphi + \left(B_{26} - \frac{D_{26}}{R}\right)\sin^2\varphi,$$

$$\beta_{22} = \left(A_{66} + \frac{B_{66}}{R}\right)\cos^2\varphi + 2A_{26}\,\cos\varphi\,\sin\varphi + \left(A_{22} - \frac{B_{22}}{R}\right)\sin^2\varphi,$$

$$\beta_{24} = \left(B_{16} + \frac{D_{16}}{R}\right)\cos^2\varphi + (B_{12} + B_{66})\cos\varphi\sin\varphi + \left(B_{26} - \frac{D_{26}}{R}\right)\sin^2\varphi,$$

$$\beta_{25} = \left(B_{66} + \frac{D_{66}}{R}\right)\cos^2\varphi + 2B_{26}\cos\varphi\,\sin\varphi + \left(B_{22} - \frac{D_{22}}{R}\right)\sin^2\varphi,$$

$$\beta_{33} = \left(F_{55} + \frac{H_{55}}{R}\right)\cos^2\varphi + 2F_{45}\,\cos\varphi\,\sin\varphi + \left(F_{44} - \frac{H_{44}}{R}\right)\sin^2\varphi,$$

$$\beta_{44} = D_{11}\cos^2\varphi + 2D_{16}\cos\varphi\,\sin\varphi + D_{66}\sin^2\varphi,$$

$$\beta_{45} = D_{16}\cos^2\varphi + (D_{12} + D_{66})\cos\varphi\,\sin\varphi + D_{26}\sin^2\varphi,$$

$$\beta_{55} = D_{66}\cos^2\varphi + 2D_{26}\,\cos\varphi\,\sin\varphi + D_{22}\sin^2\varphi. \tag{A.15}$$

Appendix B. Main equations of the general discrete layer model

B.1. Equilibrium equations

In this model, the previous laminate composite theory is used to express for each layer the internal stress forces in terms of the layer' five displacement variables and mechanical properties. However, this time the integral limits h^i_{uk} and h^i_{lk} in relations (A.1) and (A.2) are computed using the following relations:

$$h^i_{uk} = z_{i-1} + \sum_{j=1}^{k} h^i_j, \quad h^i_{lk} = z_{i-1} + \sum_{j=0}^{k-1} h^i_j, \tag{B.1}$$

where h^i_j is the thickness of the lamina j of layer i ($h^i_0 = 0$). Moreover, since a discrete layer theory is used, no shear corrections coefficients are required.

Next, the dynamic equilibrium equations of the shell, accounting for the interlayer continuity forces are written. After appropriate algebraic manipulations, the following system of equation is found:

$$\begin{aligned}
&\left[\left(A_{11} + \frac{B_{11}}{R}\right)u_{,xx} + 2A_{16}u_{,xy} + \left(A_{66} - \frac{B_{66}}{R}\right)u_{,yy} + \left(A_{16} + \frac{B_{16}}{R}\right)v_{,xx}\right.\\
&\quad + (A_{12} + A_{66})v_{,xy} + \left(A_{26} - \frac{B_{26}}{R}\right)v_{,yy} + \left(B_{11} + \frac{D_{11}}{R}\right)\varphi_{x,xx} + 2B_{16}\varphi_{x,xy}\\
&\quad + \left(B_{66} - \frac{D_{66}}{R}\right)\varphi_{x,yy} + \left(B_{16} + \frac{D_{16}}{R}\right)\varphi_{y,xx} + (B_{12} + B_{66})\varphi_{y,xy} + \left(B_{26} - \frac{D_{26}}{R}\right)\varphi_{y,yy}
\end{aligned}$$

$$+\frac{A_{12}}{R}\,w_{,x}+\left(\frac{A_{26}}{R}-\frac{B_{26}}{R^2}\right)w_{,y}\Bigg]^{i}+F_x^i-F_x^{i-1}+\left(\left(m_s+\frac{I_{z2}}{R}\right)u+\left(\frac{I_z}{R}+I_{z2}\right)\varphi_x\right)^{i}\omega^2=0.$$

$$\begin{aligned}&\Bigg[\left(A_{16}+\frac{B_{16}}{R}\right)u_{,xx}+(A_{12}+A_{66})u_{,xy}+\left(A_{26}-\frac{B_{26}}{R}\right)u_{,yy}\\&\quad+\left(A_{66}+\frac{B_{66}}{R}\right)v_{,xx}+2A_{26}v_{,xy}+\left(A_{22}-\frac{B_{22}}{R}\right)v_{,yy}+\left(B_{16}+\frac{D_{16}}{R}\right)\varphi_{x,xx}\\&\quad+(B_{12}+B_{66})\varphi_{x,xy}+\left(B_{26}-\frac{D_{26}}{R}\right)\varphi_{x,yy}+\left(B_{66}+\frac{D_{66}}{R}\right)\varphi_{y,xx}\\&\quad+2B_{26}\varphi_{y,xy}+\left(B_{22}-\frac{D_{22}}{R}\right)\varphi_{y,yy}+\left(\frac{A_{26}}{R}+\frac{F_{45}}{R}\right)w_{,x}\\&\quad+\left(\frac{A_{22}}{R}-\frac{B_{22}}{R^2}+\frac{F_{44}}{R}-\frac{H_{44}}{R^2}\right)w_{,y}-\left(\frac{F_{44}}{R^2}-\frac{H_{44}}{R^3}\right)v+\frac{F_{45}}{R}\,\varphi_x+\left(\frac{F_{44}}{R}-\frac{H_{44}}{R^2}\right)\varphi_y\Bigg]^{i}\\&\quad+F_y^i-F_y^{i-1}+\left(\left(m_s+\frac{I_{z2}}{R}\right)v+\left(\frac{I_z}{R}+I_{z2}\right)\varphi_y\right)^{i}\omega^2=0,\end{aligned}$$

$$\begin{aligned}&\Bigg[\left(F_{55}+\frac{H_{55}}{R}\right)w_{,xx}+2F_{45}w_{,xy}+\left(F_{44}-\frac{H_{44}}{R}\right)w_{,yy}-\frac{A_{12}}{R}\,u_{,x}-\left(\frac{A_{26}}{R}-\frac{B_{26}}{R^2}\right)u_{,y}\\&\quad-\left(\frac{A_{26}}{R}+\frac{F_{45}}{R}\right)v_{,x}-\left(\frac{A_{22}}{R}-\frac{B_{22}}{R^2}+\frac{F_{44}}{R}-\frac{H_{44}}{R^2}\right)v_{,y}\\&\quad-\left(\frac{B_{12}}{R}-F_{55}-\frac{H_{55}}{R}\right)\varphi_{x,x}-\left(\frac{B_{26}}{R}-\frac{D_{26}}{R^2}-F_{45}\right)\varphi_{x,y}-\left(\frac{B_{26}}{R}-F_{45}\right)\varphi_{y,x}\\&\quad-\left(\frac{B_{22}}{R}-\frac{D_{22}}{R^2}-F_{44}+\frac{H_{44}}{R}\right)\varphi_{y,y}-\left(\frac{A_{22}}{R}-\frac{B_{22}}{R^3}\right)w\Bigg]^{i}+F_z^i-F_z^{i-1}+(m_sw)^i\omega^2=0,\end{aligned}$$

$$\begin{aligned}&\Bigg[\left(B_{11}+\frac{D_{11}}{R}\right)u_{,xx}+2B_{16}u_{,xy}+\left(B_{66}-\frac{D_{66}}{R}\right)u_{,yy}+\left(B_{16}+\frac{D_{16}}{R}\right)v_{,xx}+(B_{12}+B_{66})v_{,xy}\\&\quad+\left(B_{26}-\frac{D_{26}}{R}\right)v_{,yy}+D_{11}\varphi_{x,xx}+2D_{16}\varphi_{x,xy}+D_{66}\varphi_{x,yy}\\&\quad+D_{16}\varphi_{y,xx}+(D_{12}+D_{66})\varphi_{y,xy}+D_{26}\varphi_{y,yy}+\left(\frac{B_{12}}{R}-F_{55}-\frac{H_{55}}{R}\right)w_{,x}\\&\quad+\left(\frac{B_{26}}{R}-\frac{D_{26}}{R^2}-F_{45}\right)w_{,y}+\frac{F_{45}}{R}\,v-\left(F_{55}+\frac{H_{55}}{R}\right)\varphi_x-F_{45}\varphi_y\Bigg]^{i}\\&\quad+z^iF_x^i-z^{i-1}F_x^{i-1}+\left(I_z\left(\varphi_x+\frac{u}{R}\right)+I_{z2}u\right)^{i}\omega^2=0,\end{aligned}$$

$$\left[\left(B_{16}+\frac{D_{16}}{R}\right)u_{,xx}+(B_{12}+B_{66})u_{,xy}+\left(B_{26}-\frac{D_{26}}{R}\right)u_{,yy}\right.$$
$$+\left(B_{66}+\frac{D_{66}}{R}\right)v_{,xx}+2B_{26}v_{,xy}+\left(B_{22}-\frac{D_{22}}{R}\right)v_{,yy}$$
$$+D_{16}\varphi_{x,xx}+(D_{12}+D_{66})\varphi_{x,xy}+D_{26}\varphi_{x,yy}$$
$$+D_{66}\varphi_{y,xx}+2D_{26}\varphi_{y,xy}+D_{22}\varphi_{y,yy}+\left(\frac{B_{26}}{R}-F_{45}\right)w_{,x}$$
$$-\left(\frac{B_{22}}{R}-\frac{D_{22}}{R^2}-F_{44}+\frac{H_{44}}{R}\right)w_{,y}+\left(\frac{F_{44}}{R}-\frac{H_{44}}{R^2}\right)v-F_{45}\varphi_x$$
$$\left.-\left(F_{44}-\frac{H_{44}}{R}\right)\varphi_y\right]^i+z^iF_y^i-z^{i-1}F_y^{i-1}+\left(I_z\left(\varphi_y+\frac{v}{R}\right)+I_{z2}v\right)^i\omega^2=0. \tag{B.2}$$

The different coefficients in this system are given in Eq. (A.8)

B.2. Dispersion equation matrices

The matrices $[A_0]$, $[A_1]$, $[A_2]$ used in Eq. (15) are real square matrices of dimension $5N+3(N-1)$ defined as follows:

$$[A_0]=\begin{bmatrix}
[A_0]^1 & 0 & 0 & 0 & 0 & 0 & [F_0]^1 & 0 & 0 & 0 & 0 & 0\\
 & [A_0]^2 & 0 & 0 & 0 & 0 & -[F_0]^1 & [F_0]^2 & 0 & 0 & 0 & 0\\
 & & [A_0]^3 & 0 & 0 & 0 & 0 & -[F_0]^2 & [F_0]^3 & 0 & 0 & 0\\
 & & & \ddots & 0 & 0 & 0 & 0 & 0 & \ddots & 0 & 0\\
 & & & & [A_0]^{N-1} & 0 & 0 & 0 & 0 & 0 & -[F_0]^{N-2} & [F_0]^{N-1}\\
 & & & & & [A_0]^N & 0 & 0 & 0 & 0 & 0 & -[F_0]^{N-1}\\
 & & & & & & 0 & 0 & 0 & 0 & 0 & 0\\
 & & & & & & & 0 & 0 & 0 & 0 & 0\\
 & & \text{sym} & & & & & & 0 & 0 & 0 & 0\\
 & & & & & & & & & 0 & 0 & 0\\
 & & & & & & & & & & 0 & 0\\
 & & & & & & & & & & & 0
\end{bmatrix}$$

$$[A_1] = \begin{bmatrix} [A_1]^1 & 0 & 0 & 0 & 0 \\ 0 & [A_1]^2 & 0 & 0 & 0 \\ 0 & 0 & \ddots & 0 & 0 \\ 0 & 0 & 0 & [A_1]^N & 0 \\ 0 & 0 & 0 & 0 & [0] \end{bmatrix}, \quad [A_2] = \begin{bmatrix} [A_2]^1 & 0 & 0 & 0 & 0 \\ 0 & [A_2]^2 & 0 & 0 & 0 \\ 0 & 0 & \ddots & 0 & 0 \\ 0 & 0 & 0 & [A_2]^N & 0 \\ 0 & 0 & 0 & 0 & [0] \end{bmatrix}, \tag{B.3}$$

where

$$[A_0]^i = \begin{bmatrix} a_{11} & 0 & 0 & a_{14} & 0 \\ 0 & a_{22} & 0 & a_{24} & a_{25} \\ 0 & 0 & a_{33} & 0 & 0 \\ a_{14} & a_{24} & 0 & a_{44} & a_{45} \\ 0 & a_{25} & 0 & a_{45} & a_{55} \end{bmatrix}^i,$$

$$[F_0]^i = \begin{bmatrix} 1 & 0 & 0 \\ 0 & 1 & 0 \\ 0 & 0 & 1 \\ z^i & 0 & 0 \\ 0 & z^i & 0 \end{bmatrix}, \quad [A_1]^i = \begin{bmatrix} 0 & 0 & \alpha_{13} & 0 & 0 \\ 0 & 0 & \alpha_{23} & 0 & 0 \\ -\alpha_{13} & -\alpha_{23} & 0 & \alpha_{34} & \alpha_{35} \\ 0 & 0 & -\alpha_{34} & 0 & 0 \\ 0 & 0 & -\alpha_{35} & 0 & 0 \end{bmatrix}^i,$$

$$[A_2]^i = \begin{bmatrix} \beta_{11} & \beta_{12} & 0 & \beta_{14} & \beta_{15} \\ \beta_{12} & \beta_{22} & 0 & \beta_{24} & \beta_{25} \\ 0 & 0 & \beta_{33} & 0 & 0 \\ \beta_{14} & \beta_{24} & 0 & \beta_{44} & \beta_{45} \\ \beta_{15} & \beta_{25} & 0 & \beta_{45} & \beta_{55} \end{bmatrix}^i \tag{B.4}$$

with coefficients $a^i_{\gamma\delta}\,\alpha^i_{\gamma\delta}$ and $\beta^i_{\gamma\delta}$ defined as follows:

$$\begin{aligned} &a^i_{11} = \left(m_s + \frac{I_{z2}}{R}\right)\omega^2, \quad a^i_{14} = \left(\frac{I_z}{R} + I_{z2}\right)\omega^2, \quad a^i_{22} = \left(m_s + \frac{I_{z2}}{R}\right)\omega^2 - \frac{F_{44}}{R^2} + \frac{H_{44}}{R^3}, \\ &a^i_{24} = \frac{F_{45}}{R}, \quad a^i_{25} = \frac{F_{44}}{R} - \frac{H_{44}}{R^2} + \left(\frac{I_z}{R} + I_{z2}\right)\omega^2, \quad a^i_{33} = \left(m_s + \frac{I_{z2}}{R}\right)\omega^2 - \frac{A_{22}}{R^2} + \frac{B_{22}}{R^3}, \\ &a^i_{44} = I_z\omega^2 - F_{55} - \frac{H_{55}}{R}, \quad a^i_{45} = -F_{45}, \quad a^i_{55} = I_z\omega^2 - F_{44} - \frac{H_{44}}{R}, \end{aligned} \tag{B.5}$$

$$\alpha_{13}^{i} = -\left(\frac{A_{12}}{R}\right)^{i} \cos\varphi - \left(\frac{A_{26}}{R} - \frac{B_{26}}{R^2}\right)^{i} \sin\varphi,$$

$$\alpha_{23}^{i} = -\left(\frac{A_{22}}{R} - \frac{B_{22}}{R^2} + \frac{F_{44}}{R} - \frac{H_{44}}{R^2}\right)^{i} \sin\varphi - \left(\frac{A_{26}}{R} + \frac{F_{45}}{R}\right)^{i} \cos\varphi,$$

$$\alpha_{34}^{i} = \left(\frac{B_{12}}{R} - F_{55} - \frac{H_{55}}{R}\right)^{i} \cos\varphi + \left(\frac{B_{26}}{R} - \frac{D_{26}}{R^2} - F_{45}\right)^{i} \sin\varphi,$$

$$\alpha_{35}^{i} = \left(\frac{B_{22}}{R} - \frac{D_{22}}{R^2} - F_{44} + \frac{H_{44}}{R}\right)^{i} \sin\varphi + \left(\frac{B_{26}}{R} - F_{45}\right)^{i} \cos\varphi \tag{B.6}$$

and

$$\beta_{11}^{i} = \left(A_{11} + \frac{B_{11}}{R}\right)^{i} \cos^2\varphi + 2A_{16}^{i} \cos\varphi \sin\varphi + \left(A_{66} - \frac{B_{66}}{R}\right)^{i} \sin^2\varphi,$$

$$\beta_{12}^{i} = \left(A_{16} + \frac{B_{16}}{R}\right)^{i} \cos^2\varphi + (A_{12} + A_{66})^{i} \cos\varphi \sin\varphi + \left(A_{26} - \frac{B_{26}}{R}\right)^{i} \sin^2\varphi,$$

$$\beta_{14}^{i} = \left(B_{11} + \frac{D_{11}}{R}\right)^{i} \cos^2\varphi + 2B_{16}^{i} \cos\varphi \sin\varphi + \left(B_{66} - \frac{D_{66}}{R}\right)^{i} \sin^2\varphi,$$

$$\beta_{15}^{i} = \left(B_{16} + \frac{D_{16}}{R}\right)^{i} \cos^2\varphi + (B_{12} + B_{66})^{i} \cos\varphi \sin\varphi + \left(B_{26} - \frac{D_{26}}{R}\right)^{i} \sin^2\varphi,$$

$$\beta_{22}^{i} = \left(A_{66} + \frac{B_{66}}{R}\right)^{i} \cos^2\varphi + 2A_{26}^{i} \cos\varphi \sin\varphi + \left(A_{22} - \frac{B_{22}}{R}\right)^{i} \sin^2\varphi,$$

$$\beta_{24}^{i} = \left(B_{16} + \frac{D_{16}}{R}\right)^{i} \cos^2\varphi + (B_{12} + B_{66})^{i} \cos\varphi \sin\varphi + \left(B_{26} - \frac{D_{26}}{R}\right)^{i} \sin^2\varphi,$$

$$\beta_{25}^{i} = \left(B_{66} + \frac{D_{66}}{R}\right)^{i} \cos^2\varphi + 2B_{26}^{i} \cos\varphi \sin\varphi + \left(B_{22} - \frac{D_{22}}{R}\right)^{i} \sin^2\varphi,$$

$$\beta_{33}^{i} = \left(F_{55} + \frac{H_{55}}{R}\right)^{i} \cos^2\varphi + 2F_{45}^{i} \cos\varphi \sin\varphi + \left(F_{44} - \frac{H_{44}}{R}\right)^{i} \sin^2\varphi,$$

$$\beta_{44}^{i} = D_{11}^{i} \cos^2\varphi + 2D_{16}^{i} \cos\varphi \sin\varphi + D_{66}^{i} \sin^2\varphi,$$

$$\beta_{45}^{i} = D_{16}^{i} \cos^2\varphi + (D_{12} + D_{66})^{i} \cos\varphi \sin\varphi + D_{26}^{i} \sin^2\varphi,$$

$$\beta_{55}^{i} = D_{66}^{i} \cos^2\varphi + 2D_{26}^{i} \cos\varphi \sin\varphi + D_{22}^{i} \sin^2\varphi. \tag{B.7}$$

References

[1] L.R. Koval, On sound transmission into an orthotropic shell, *Journal of Sound and Vibration* 63 (1) (1979) 51–59.
[2] H.C. Nelson, B. Zapatowski, M. Bernstein, Vibration analysis of orthogonally stiffened circular fuselage and comparison with experiment, *Proceedings of the Institute of Aeronautical Sciences National Specialist's Meeting on Dynamics and Aeroelasticity*, 1958, pp. 77–87.

[3] L.R. Koval, Sound transmission into a laminated composite cylindrical shell, *Journal of Sound and Vibration* 71 (4) (1980) 523–530.
[4] C.W. Bert, J.L. Baker, D.M. Egle, Free vibrations of multilayer anisotropic cylindrical shells, *Journal of Composite Materials* 3 (1969) 480–499.
[5] A. Blaise, C. Lesueur, On the sound transmission into an orthotropic infinite shell: comparison with Koval's results and understanding of phenomena, *Journal of Sound and Vibration* 150 (2) (1991) 233–243.
[6] A. Blaise, C. Lesueur, Acoustic transmission through a 2-D orthotropic multi-layered infinite cylindrical shell, *Journal of Sound and Vibration* 155 (1) (1992) 95–109.
[7] A. Blaise, C. Lesueur, Acoustic transmission through a "3-D" orthotropic multi-layered infinite cylindrical shell, part I: formulation of the problem, *Journal of Sound and Vibration* 171 (5) (1994) 651–664.
[8] K.H. Heron, Curved laminates and sandwich panels within predictive SEA, in: *Proceedings of the Second International AutoSEA Users Conference*, Detroit, USA, 2002.
[9] A.W. Leissa, *Vibrations of Shells*, NASA SP 288, U.S. Government Printing Office, Washington DC, 1973.
[10] J.-M. Berthelot, *Matériaux Composites—Comportement Mécanique et Analyse des Structures*, Editions TEC & DOC, Paris, 1999.
[11] C. Lesueur, *Rayonnement Acoustique des Structures—Vibroacoustique, Interactions Fluid–Structure*, Editions Eyrolles, Paris, 1988.
[12] M. Abramowitz, I.A. Stegun, *Handbook of Mathematical Functions with Formulas, Graphs and Mathematical Tables*, Dover Publications, New York, 1972.
[13] A. Blaise, C. Lesueur, Acoustic transmission through a "3-D" orthotropic multi-layered infinite cylindrical shell, part II: validation and numerical exploitation for large structures, *Journal of Sound and Vibration* 171 (5) (1994) 665–680.
[14] N. Atalla, S. Ghinet, H. Osman, Transmission loss of curved composite panels with acoustic materials, in: *Proceedings of the 18th International Congress on Acoustics (ICA)*, Kyoto, 2004.
[15] J.-L. Batoz, G. Dhatt, *Modélisation des Structures par Éléments Finis*, Hermes, Paris, 1990.
[16] D. Guy, *Matériaux Composites*, Hermes, Paris, 1997.